Establishing *In Vitro* Organoid-Based Epithelial-Mesenchymal Transition Model in Cholangiocarcinoma Including Tumor Extracellular Environment

Towards a More Representative In Vitro Model

Huyen My Nguyen
Master Thesis
Biomedical Engineering

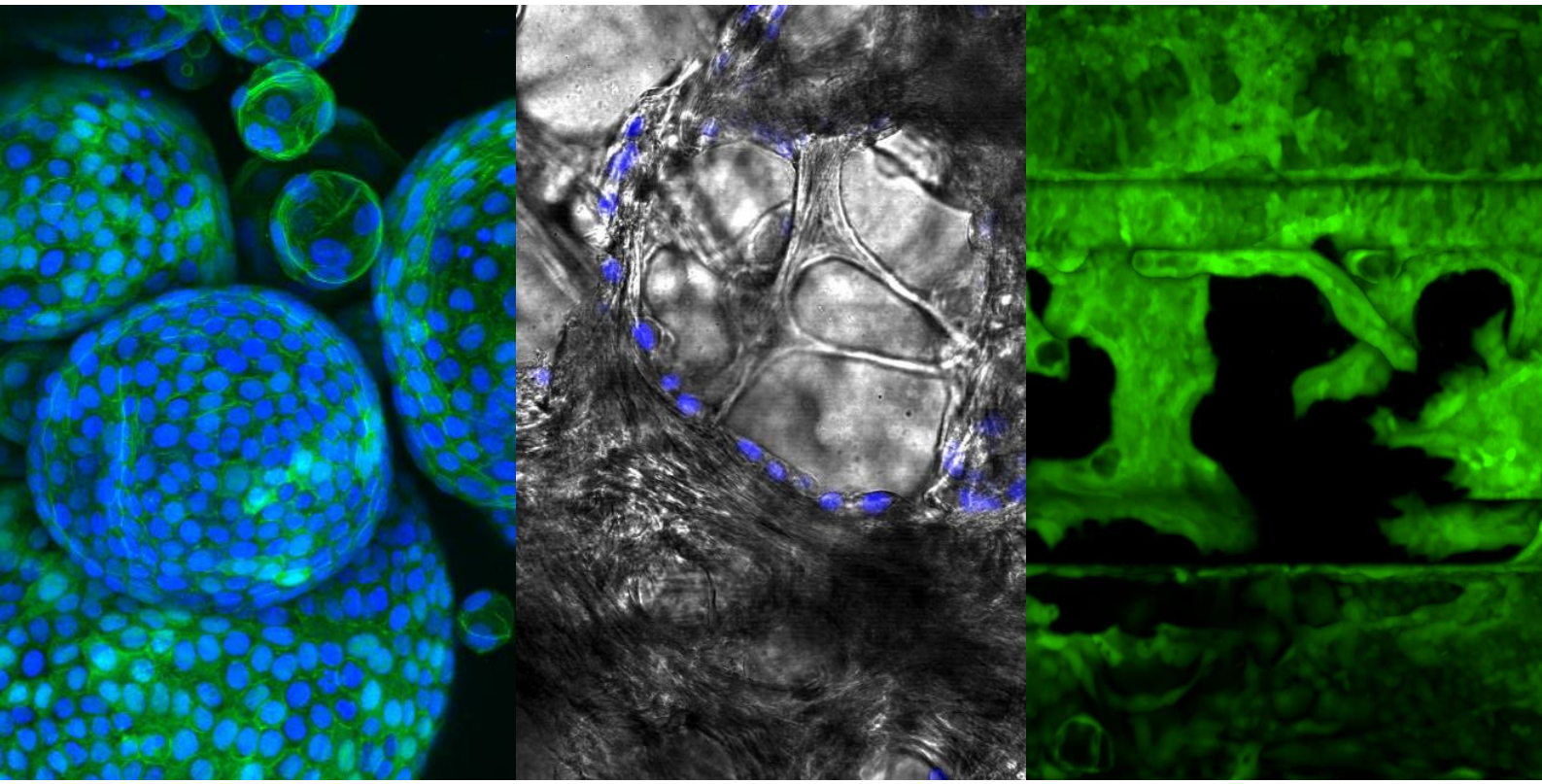

TU Delft Delft University of Technology

Erasmus MC Universitair Medisch Centrum Rotterdam

Establishing *In Vitro* Organoid-Based Epithelial-Mesenchymal Transition Model in Cholangiocarcinoma Including Tumor Extracellular Environment

Towards a More Representative In Vitro Model

Master Thesis

By

Huyen My Nguyen

to obtain the degree of Master of Science
at the Delft University of Technology,
to be defended publicly on Friday, April 30, 2021 at 10am.

Student number	4430786
Supervisors:	Dr. M.M.A. Verstegen, Erasmus MC
	Dr. Ir. E.L. Fratila-Apachitei, TU Delft
	Prof. Dr. A.A. Zadpoor, TU Delft, chair of the exam committee
Daily supervisor:	G.S. van Tienderen

ABSTRACT

Cholangiocarcinoma (CCA) is a highly aggressive biliary tumor with a poor prognosis and limited treatment options. Various critical aspects of CCA development remain unclear. Lately, the dynamic process of epithelial-mesenchymal transition (EMT) was highlighted to play a crucial role in the fundamental mechanism of metastatic dissemination. However, *in vitro* EMT studies are mainly limited to conventional 2D models which lack *in vivo* tumor physiology. Recently, 3D organoid culture methods provide us new model possibilities. Therefore, our research aim was to establish a representative *in vitro* organoid-based epithelial-mesenchymal transition model in cholangiocarcinoma including its *in vivo* pathophysiology and tumor microenvironment. This study focusses on three different aspects of the tumor microenvironment regarding EMT activation in CCA organoids:

1. **The effects of EMT promoting growth factors and culture media on EMT activation.** Various growth factors are highlighted to play a crucial role in EMT activation in different cancer types. To study EMT activation in CCA, various growth factors were added to CCA organoids. We observed round shaped organoid structures consisting of single layered epithelium for all conditions. Additionally, gene expression levels of EMT related markers were increased for specific growth factor conditions. The use of various culture media combined with transforming growth factor β1 (TGF-β1) showed the most substantial differences in mRNA expression of EMT markers in branching medium (BM). Based on these results, specific growth factors and BM were used to find the optimal culture conditions to induce EMT. Although we did not find significant morphological differences between the various conditions, altered gene expression levels of EMT markers were observed after TGF-β1 and tumor necrosis factor alpha (TNF-α) treatment in BM.
2. **The effect of the tumor extracellular matrix on EMT activation.** The tumor extracellular matrix (ECM) is an important component of the tumor microenvironment that stimulates the malignant behavior of surrounding cells. The combination of CCA organoids and patient-derived ECM resulted in morphological changes. Cells with a polygonal shape adopted an irregular shape after TGF-β1 treatment. On top of that, our data revealed that patient-specific ECM and CCA organoids altered the gene expression of EMT related markers.
3. **The effect of the interstitial fluid flow on EMT activation**. The use of a microfluidic platform enabled us to study the effect of fluid flow on EMT *in vitro*. Cells formed organoid structures in the absence and the presence of a fluid flow. However, cells only migrated to the surrounding culture medium due to the presence of a fluid flow. When cells were seeded directly into the chip, cells formed a tube structure with protrusions growing outwards. The protrusions growth was accelerated by the addition of TGF-β1 and led to increased cell migration. Additionally, fluid flow conditions resulted in altered gene expression levels of EMT related markers. Our data suggest that fluid flow could potentially stimulate EMT in CCA organoids.

Overall, our findings have demonstrated that growth factors, native ECM and interstitial fluid flow could be used to induce EMT *in vitro*. Indicating that the tumor microenvironment plays a crucial role in EMT and tumor progression. Our novel *in vitro* CCA organoid-based EMT model provides a foundation towards a more representative EMT *in vitro* model to unravel the underlying mechanism of CCA and its progression.

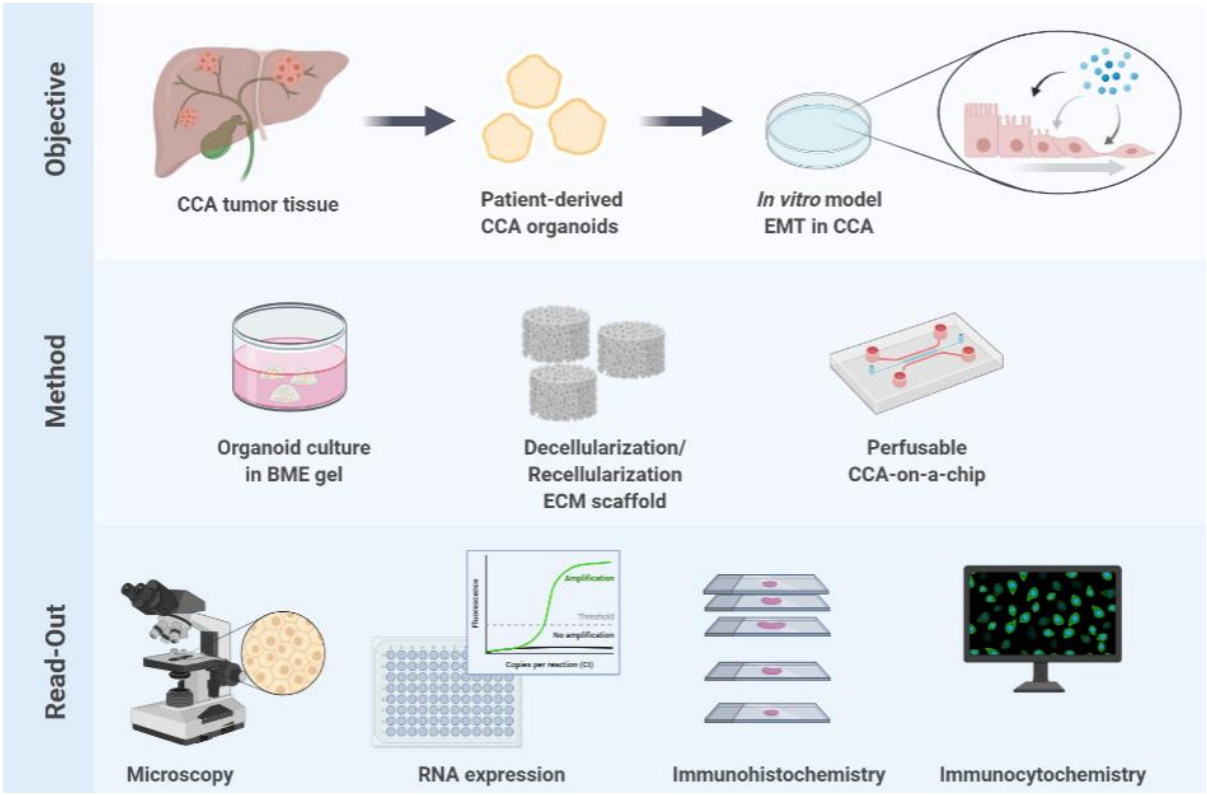

Figure 1. Graphical abstract.

CONTENTS

1

INTRODUCTION

Primary liver cancer (PLC) is worldwide one of the most lethal malignancies with 841,000 new incidences and 782,000 deaths each year [3, 4]. The major PLC subtypes are hepatocellular carcinoma (HCC), which represents ~75% of all PLC, and cholangiocarcinoma (CCA) which accounts for ~15% of all PLC [1]. HCC develops from hepatocytes, which are liver parenchymal cells, while CCA develops from cholangiocytes, which are epithelial cells of the biliary tract. CCA is a highly heterogeneous aggressive biliary malignant tumor with a 5-year survival rate of ~5-10% [1, 5]. CCA has two main subtypes: intrahepatic CCA (iCCA) and extrahepatic CCA (eCCA) [6]. iCCA originates from small bile ducts and bile ductules, while eCCA emerges from the hilum to the distal part of the large bile ducts (Figure 2).

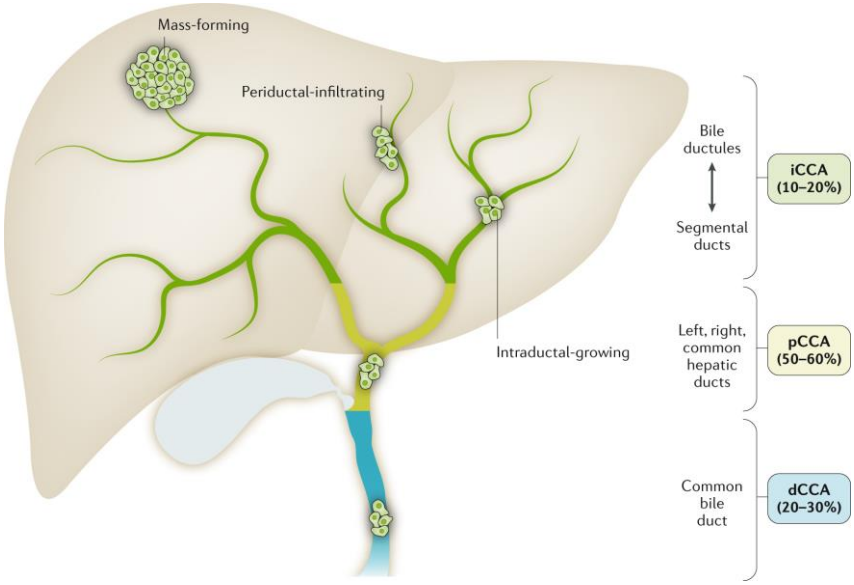

Figure 2. A schematic representation of cholangiocarcinoma (CCA). CCA is an aggressive tumor which arises from the bile duct. CCA has two main subtypes: intrahepatic CCA (iCCA) and extrahepatic CCA (eCCA) which includes perihilar CCA (pCCA) and distal CCA (dCCA) [1].

The silent clinical presentation of CCA complicates its diagnosis. ~70% of CCA patients are diagnosed at a late clinical stage with a poor prognosis [7]. Although surgical intervention is the only curative treatment option, only ~25% of CCA patients are eligible for resection with a relapse rate of 60% [8]. Moreover, pharmalogical treatments are not effective for the majority of patients [9]. The mechanism of chemoresistance in CCA patients still remains unresolved due to the lack of a representative model which recapitulates the complete native tumor. Most preclinical CCA studies are based on two-dimensional (2D) cell lines or mouse models [10]. Although invaluable information regarding CCA was obtained using these *in vivo* and *in vitro* models, various critical characteristics of CCA invasion and its progression are still poorly understood. Therefore, it is necessary to develop a representative *in vitro* CCA model which includes the pathophysiology of the initial tumor to understand the underlying mechanism of CCA patient-specific chemoresistance and progression.

Lately, studies have focused on the dynamic process of cancer-associated epithelial-mesenchymal transition (EMT) to unravel the fundamental mechanism of metastatic dissemination [9]. EMT is a reversible process in which epithelial cells undergo phenotype changes and gradually adopt more mesenchymal-like characteristics (Figure 3) [2, 11]. Cells lose their cell-cell interaction, apico-basal polarity, and cobblestone-like cell shape. However, these cells gain invasive properties, front-back polarity and spindle-like cell shape along with major cellular changes in EMT transcription factors, epigenetic modifications and post-translational modifications of proteins [2, 9].

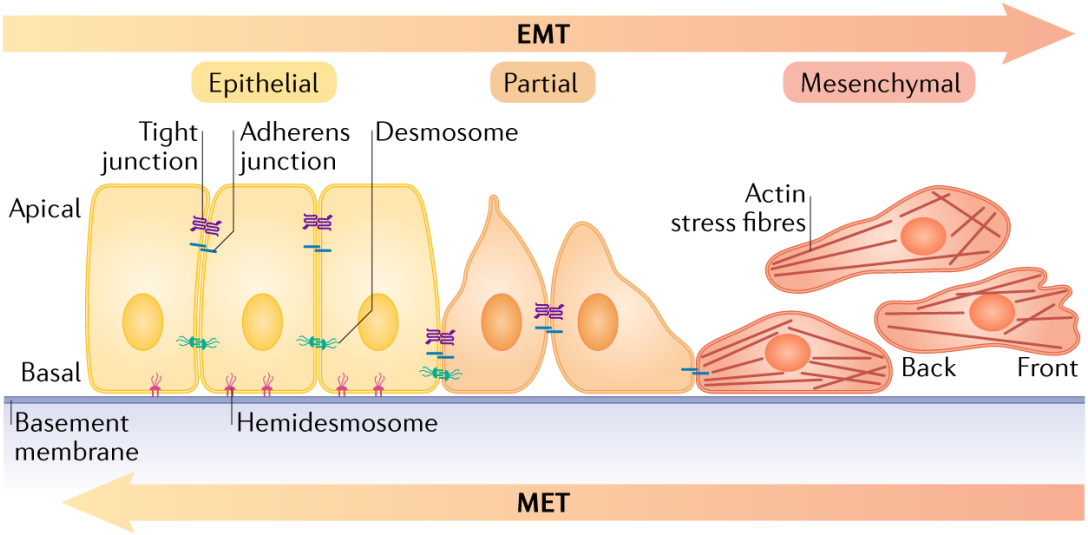

Figure 3. The reversible epithelial-mesenchymal transition process (EMT). The epithelial cells partially or fully undergo EMT and gradually adopt more mesenchymal-like phenotypes. These cells lose their cell-cell interaction, apico-basal polarity, and cobblestone-like cell shape, while they gain invasive properties, spindle-like cell shape and front-back polarity [2].

The major cellular changes can be triggered by the tumor microenvironment which consists of cellular and non-cellular components. Cellular components such as cancer-associated fibroblasts (CAFs) and tumor-associated macrophages (TAMs) secrete various signaling molecules into the tumor microenvironment which could stimulate malignant behavior of tumor cells. One of the major EMT promoting signaling molecules is transforming growth factor β1 (TGF-β1). TGF-β1 activates a plethora of signaling pathways resulting in the initiation of transcription factors that regulate gene expression related to EMT [12]. Various clinical studies have demonstrated that the overexpression of TGF-β1 was associated with tumor invasion, progression and poor prognosis in various cancer types including CCA [12, 13]. Additionally, *in vitro* studies induced EMT in CCA cell lines with TGF-β1 treatment resulting in morphological changes, altered EMT gene expressions, cell migration and invasion [14, 15].

The extracellular matrix (ECM) is a non-cellular component of the tumor microenvironment that consists of many different molecules such as cytokines, macromolecules, remodeling proteins and matrix metalloproteinases (MMPs). The ECM does not only function as a structural scaffold, but also provides biochemical and biomechanical cues that regulate the behavior of surrounding cells [16]. Consequently, the ECM plays an essential role in promoting malignant behavior of tumor cells in a tumor microenvironment. Particularly, the desmoplastic extracellular environment of CCA, which mainly consist of collagen type I and fibronectin, results in an increased rigidity of the ECM. Whilst rigidity of healthy ECM provides tumor suppressor functions, an increased rigidity of ECM could stimulate the malignant behavior of tumor cells by delivering a wide variety of signals to cells [17, 18]. Importantly, the influence of the ECM composition is also involved in promoting EMT to facilitate invasion and metastasis [16].

However, most *in vitro* studies regarding EMT in CCA were based on 2D cell line models [15, 19, 20]. Although 2D cell lines are easy to culture, this culture method lacks three-dimensional (3D) spatial architecture, cell-cell interaction and interaction with the tumor microenvironment [17]. Additionally, CCA is a highly heterogeneous tumor, while cell lines represent a single cell which can also diverge from the original tumor over time due to the selectivity of culture medium [17]. To further advance research on CCA progression, different culture methods should be considered for *in vitro* modeling of EMT in CCA.

Recently, a novel organoid culture method was established which enables to recapitulate the structural and functional characteristics of the original tissue *in vitro* [21]. Organoids are self-organizing 3D structures derived from patient-specific cells. Broutier et al. [10] have successfully cultured organoids derived from CCA patients. These organoids mimic cell-cell interactions, cell-matrix interactions and cellular heterogeneity of CCA [17]. In contrast to cell lines, CCA organoids maintain their heterogeneity after long-term expansion [22]. Furthermore, organoids could not only aid in understanding the nature of CCA, but could also play an essential role in drug testing and personalized medicine [10]. To date, an organoid-based epithelial-mesenchymal transition (OEMT) model for intestinal fibrosis has been established by Hahn et al. [23]. However, an OEMT model for CCA does not exist yet.

Although organoids mimic the architecture and function of the initial tumor accurately, the tumor microenvironment is not included in this culture method. Organoids are mainly cultured in basement membrane matrix (BME) which is derived from mouse sarcoma basement membrane and do not mimic the characteristics of the tumor specific extracellular matrix (ECM) [24]. Previous tumor-derived ECM research in our lab successfully obtained cell-free ECM scaffolds of CCA tissue using decellularization techniques [25]. Decellularization enables isolation of the ECM from tissue, while preserving all structural and functional properties of the ECM [26]. After the decellularization process, the cell-free ECM scaffolds were recellularized with CCA organoids to study the critical role of the ECM in CCA

progression [25]. Currently, there is no 3D *in vitro* EMT model of CCA that includes the ECM and its original biochemical and biomechanical properties. Further investigation into the relationship between EMT and ECM could provide more insight on EMT and CCA development.

Besides the ECM of the tumor, the interstitial fluid flow is another critical aspect in tumor progression which is not included in the current organoid culture method. Organoids are mainly cultured in BME/matrigel under static conditions. However, the altered fluidic stream in the tumor contributes to the change in biomechanical cues in the tumor microenvironment which leads to EMT initiation and increased tumor invasion [27]. Therefore, multiple studies highlighted the significance of the effect of interstitial fluid flow on tumor invasion and metastasis in various cancer types [28, 29]. Since the interest has grown in the effect of the fluid flow, major advances have been made in developing *in vitro* organ-on-a-chip microfluidic models which mimic the fluid flow *in vivo*. Noteworthy, a flow-induced epithelial-mesenchymal transition model for ovarian cancer has been developed by Rizvi, et al. [30]. Furthermore, a gut-on-a-chip model has been established using human intestinal organoids [31]. However, there is no flow-induced epithelial-mesenchymal transition model developed for CCA organoids. A better understanding of the interaction between EMT and fluid flow may provide new insight in the mechanism of EMT in CCA and possible novel treatment options for CCA patients.

The overarching aim of this project is to establish a novel *in vitro* organoid-based epithelial-mesenchymal transition model in cholangiocarcinoma. To develop a more representative *in vitro* EMT model for CCA organoids, we will investigate the following three aspects of the tumor microenvironment:

1. *What are the effects of different EMT promoting growth factors and culture media on the activation of EMT in CCA organoids cultured in BME?*

To investigate the effect of different growth factors and culture media on EMT induction, CCA organoids will be cultured in BME with different culture media including expansion medium (EM), tumor differentiation medium (TDM) and branching medium (BM). Different concentrations of the growth factors will be added to the medium to promote EMT. The following growth factors will be used*:* transforming growth factor β1 (TGF-β1), tumor necrosis factor α (TNF-α), and interleukin-6 (IL-6).

2. *What is the effect of the tumor extracellular matrix on EMT activation in CCA organoids?*

The effect of the ECM on EMT initiation in CCA will be investigated by culturing CCA organoids in ECM scaffolds. To obtain tumor-derived and donor ECM scaffolds, tissue will be decellularized by removing the cells from the ECM structure. Subsequently, the ECM scaffolds will be recellularized by culturing CCA organoids in the ECM scaffold. EMT in CCA organoids on the ECM scaffolds will be induced by adding TGF-β1 and TNF-α to the culture medium.

3. *What is the effect of the interstitial fluid flow on EMT activation in CCA organoids?*

To establish a flow-induced EMT model in CCA organoids, we will make use of a microfluidic platform developed by Mimetas [32]. The OrganoPlate is an organ-on-a-chip model which enables gravity-driven perfusion and barrier-free definition of culture matrices and cells in 3D [32]. CCA organoids will be cultured in a 3-lane OrganoPlate with a flow rate and TGF-β1 treatment.

To assess the effect of the three aspects of the tumor extracellular environment on EMT initiation in CCA organoids, different read-out methods will be used such as cell morphology, gene expression, immunohistochemistry and immunocytochemistry.

2

MATERIALS & METHODS

2.1 Cell isolation and culture

CCA organoids were isolated from CCA tissue of three patients (n=3) as previously described [10], resuspended in basement membrane matrix (BME) and polymerized at 37°C and 5% CO_2. CCA organoids were cultured in expansion medium, passaged at a ratio of 1:6 to 1:8 every 7 days and used between passage 78 and 128. Expansion medium was refreshed twice a week. The expansion medium composition can be found in supplemental Table 6.

2.2 EMT promoting factors and culture media

2.2.1 EMT promoting factor treatment

CCA organoids were cultured in BME and expansion medium without A8301. One day after cell seeding, these cells were treated with different concentrations and combinations of TGF-β1 (Life technologies), TNF-α (PeproTech) and IL-6 (Thermofisher) for 7 days (Table 1). The culture medium was refreshed every 3 days.

Table 1: Different growth factor treatments for CCA organoids cultured in BME.

Condition	Concentration
1	Control
2	2ng/ml TGF-β1
3	20ng/ml TGF-β1
4	20ng/ml TNF-α
5	20ng/ml TNF-α + 2ng/ml TGF-β1
6	20ng/ml TNF-α + 20ng/ml TGF-β1
7	20ng/ml IL-6
8	20ng/ml IL-6 + 2ng/ml TGF-β1
9	20ng/ml IL-6 + 20ng/ml TGF-β1

2.2.2 Different culture media

CCA organoids were cultured in BME with different culture media including expansion medium without A8301 (EM^-), tumor differentiation medium (TDM) and branching medium (BM). The composition of the media can be found in supplemental Table 6-Table 7 Different concentrations of TGF-β1 (Life technologies) were added to the culture medium for 7 days (Table 2). The culture medium was refreshed every 3 days.

Table 2: Different growth factor treatments for CCA organoids cultured in BME with different medium compositions. CCA organoids were cultured in expansion medium without A8301, tumor differentiation medium and branching medium. The growth factor concentrations were added to all medium compositions.

Condition	Concentration
1	Control
2	2ng/ml TGF-β1
3	20ng/ml TGF-β1
4	20ng/ml TNF-α + 2ng/ml TGF-β1
5	20ng/ml IL-6 + 2ng/ml TGF-β1

2.3 ECM scaffold

2.3.1 ECM scaffold source

Tumor and donor tissues were used as source for the ECM scaffolds. Tumor tissues (n=3) were obtained from partial resection of the liver of CCA patients, while donor tissues (n=3) originated from donor livers which were not suitable for transplantation. The approval of the Medical Ethical Council of the Erasmus MC and informed consents were obtained to use tissues for research purposes (MEC-2014-060). The tissues were frozen at -20ºC for at least 24h.

2.3.2 Decellularization

To obtain the ECM scaffolds, cells were removed from tissue using decellularization method. The frozen tissues were thawed for 10min and frozen again. The freeze-thaw cycle was repeated three times. Small tissue cylinder punches of 6mm diameter were obtained using a disposable biopsy punch. To remove the cells, the tissue punches were washed in a beaker on a magnetic stirrer at 1500rpm according the protocol described in
Table 3. For every step 250ml solution was used. To check whether cells were removed, DNA was isolated from ~10mg tissue before decellularization, also referred to as t=0, and after decellularization using QIAamp DNA micro kit (Qiagen). DNA isolation was carried out according to the manufacture's protocol. DNA content was determined using the Nanodrop 2000 (Thermo Fisher).

Table 3: Decellularization protocol for tissue punches.

Solution	Time
Distilled H_2O	30min
Hypertonic saline (9% NaCl)	1h
Distilled H_2O	1h
4% Triton X-100 + 1% Ammonia*	30min (repeat 20-40 times)
PBS 1x	30min
DNAse **	3h at 37ºC
PBS 1x	30min (repeat x2)

* Repeat at least 20 times or until tissue is see-through color

** DNAse 1L: 0.9% NaCL (9g), 100 mM CaCl2 (11,1g), 100 mM mgCl2 (9,52g), DNAse (12mg)

2.3.3 Scaffold preparation

Decellularized scaffold punches were embedded in optical cutting temperature (OCT) compound and cut in slices with a thickness of 200µm using a cryostat at -15°C. The scaffold slices were kept at -20°C. One day before seeding the scaffolds with cells, the scaffolds were washed three times with PBS and soaked in advanced DMEM/F12 with 10% penicillin-streptomycin (P/S), 10% primocin and 10% anti-anti overnight. Before cell seeding, the scaffolds were washed three times with advanced DMEM/F12 supplemented with 50µg/ml primocin, 1% penicillin streptomycin, 1% ultraglutamine and 10mM HEPES (DMEM/F12^{++++}). The scaffold slices were placed in the middle of a well of a 24-wells plate without medium and kept at 37°C and 5% CO_2 for 45min to dry and prepare for recellularization.

2.3.4 Recellularization

CCA organoid cells were obtained from BME droplets. To remove BME, CCA organoids were washed in cold advanced DMEM/F12^{++++} followed by centrifuging at 1500rpm for 5min at 4°C. The supernatant was removed and organoids were washed and centrifuged again. After removing the supernatant, 1ml trypsin was added for 10min at 37°C to obtain single cells. The Burker-Turk cell counting chamber was used to count single cells and advanced DMEM/F12^{++++} was added to deactivate trypsin activity. Cells were centrifuged at 1500rpm for 5min at 4°C. The supernatant was removed and the cell pellet was resuspended in expansion medium with a concentration of 30000cells/µl. 5µl cell suspension was loaded on dried scaffold slices. The scaffolds with cells were incubated at 37°C and 5% CO_2 for at least 2h before adding branching medium.

2.3.5 Growth factor treatment for cells seeded in scaffolds

One day after cell seeding in the scaffolds, 20ng/ml TGF-β1 and 20ng/ml TNF-α was added to branching medium for 21 days. The control condition only consists of branching medium. The culture medium was refreshed every 3 days.

2.4 CCA-on-a-chip

The 3-lane OrganoPlate (Mimetas, #4004-400-B) is a microfluidic platform developed by Mimetas. This platform consists of 40 chips with three flow channels in each chip. CCA organoids were seeded in three different ways on the OrganoPlate to develop a CCA-on-a-chip model.

2.4.1 In gel seeding

Single cells were obtained from CCA organoids cultured in BME by using trypsin as previously described. ~10,000 CCA organoid cells in 2.1µl BME were seeded in the middle channel the chip and polymerized for 15 min at 37°C and 5% CO_2. After polymerization, 50µl expansion medium was added to the top inlet followed by the top outlet, bottom inlet and bottom outlet. The plate was placed in an incubator (37°C, 5% CO_2) including an interval rocker (OrganoFlow L, Mimetas) with an incline of +7° and −7° and interval of 8min (121.2 µl/h). Expansion medium without A8301 was refreshed every three days. For TGF-β1 induced EMT experiments, cells were treated with 20ng/ml TGF-β1 for 8 days.

2.4.2 Gel-gel seeding

2.1µl BME was loaded in the middle channel of the chip and polymerized for 15min at 37°C and 5% CO_2. During BME polymerization, single cells were obtained from CCA organoids using trypsin as previously described. 20,000 CCA organoid cells in 2µl BME were seeded in the top channel of the chip and polymerized for 15 min at 37°C and 5% CO_2. After polymerization, 50µl expansion medium was added to the bottom inlet and outlet. The plate was placed in an incubator (37°C, 5% CO_2) including an interval rocker (OrganoFlow L, Mimetas) with an incline of +7° and −7° and interval of 8min (121.2 µl/h). Expansion medium without A8301 was refreshed every three days. For TGF-β1 induced EMT experiments, cells were treated with 20ng/ml TGF-β1 for 8 days.

2.4.3 Tubule seeding

2.1µl BME was loaded in the middle channel of the chip and polymerized for 15min at 37°C and 5% CO_2. During BME polymerization, single cells were obtained from CCA organoids using trypsin as previously described. 100,000 CCA organoid cells in 2µl expansion medium without A8301 were seeded in the top channel of the chip. The plate was placed in the incubator for 45min at a 70° angle, 37°C and 5% CO_2. After incubation, 50µl expansion medium without A8301 of was added to the top inlet. The plate was placed back into the incubator for 2h. Subsequently, all remaining inlets and outlets were loaded with 50µl medium. The plate was placed back in the incubator without an angle or a flow rate overnight. After incubation without a flow rate, the plate was placed in an incubator (37°C, 5% CO_2) including an interval rocker (OrganoFlow L, Mimetas) with an incline of +7° and −7° and interval of 8min (121.2 µl/h). Expansion medium without A8301 was refreshed every three days. For TGF-β1 induced EMT experiments, cells were treated with 20ng/ml TGF-β1 for 8 days.

2.5 Microscopy

All bright field images of the experiments were analyzed and captured using Evos FL (Life Technologies). The CCA-on-a-chip experiments with CCA1 tagged GFP organoids were also analyzed and captured using Opera Phenix system and Harmony 4.9 software.

2.6 Histology and immunohistochemistry

BME samples and ECM samples were fixated with 4% formaldehyde for 30min at room temperature. 3% agarose solution was added after fixation. The solidified agarose with cells/scaffolds were placed in a cassette for paraffin embedding. The embedded samples were cut into slices with 4µm thickness using a microtome (Adamas instruments BV.). The slices were placed on microscope glass slides and stained with hematoxylin and eosin (H&E) to visualize cell nuclei and cytoplasm, respectively. The slides containing paraffin slices were placed in a slide holder. The slices were treated with different solutions as described in Table 4. After staining, glass slides were mounted with Pertex and covered by coverslips. The slices were analyzed and captured using Zeiss Axiocam 305 color microscope camera and Zen 3.2 Blue software.

Table 4: Hematoxylin and Eosin (H&E) staining protocol for paraffin slices.

Solution	Time
Xylene	5min (repeat 2 times)
100% ethanol	5min (repeat 2 times)
96% ethanol	3min
70% ethanol	3min
Deionized water	5min
Hematoxylin	3min
Deionized water	30sec
Tap water	5min
Acid ethanol	30sec
Tap water	1min
Deionized water	2min
Eosin	1min
70% ethanol	5min
96% ethanol	5min
100% ethanol	5min (repeat 2 times)
Xylene	5min (repeat 2 times)

2.7 Immunocytochemistry

ECM slices with cells and organoids in BME were fixated with 4% formaldehyde for 30min at room temperature and prepared for immunocytochemistry. Whole mount staining was carried out using AlexaFluor 488 Phalloidin (Invtrogen), Vimentin antibody (GeneTex), AlexaFluor 488 goat anti-rabbit (Invtrogen) and/or DAPI (4′,6-diamidino-2-phenylindole, VECTASHIELD® Antifade Mounting Medium with DAPI). Samples were washed three times with PBS. 0.1% T-X100 in PBS was added for 30min. Samples were again washed three times with PBS. 5% BSA was added for 60min. Samples destined for vimentin staining were incubated with first antibody (Vimentin antibody) overnight at 4ºC. Vimentin antibody was diluted to 1:100 with 1%BSA with PBS. Note: keep the samples in the dark. Samples were washed five times with PBS and incubated with second antibody AlexaFluor 488 goat anti-rabbit (1:150) for 60min at room temperature. Samples destined for phalloidin staining were washed five times with PBS and incubated with AlexaFluor 488 Phalloidin (1:40) at room temperature. All samples were washed with PBS, incubated with DAPI for 60min at room temperature and washed again with PBS. Samples were transferred to petri dishes with ~20µl BME to keep the samples in place and covered with PBS before imaging. Confocal images were obtained using Leica SP5 AOBS with multiphoton laser and APO dipping lens

(20x) with numerical aperture of 1.00 was used. AlexaFluor 488 and AlexaFluor 488 phalloidin signal were obtained with 448nm excitation and 514nm emission. DAPI signal was obtained with 496nm excitation and 458nm emission. Images were captured with 512 or 1024 pixel resolution and 2.5µm or 5µm z-step size. The maximum intensity projection images were obtained using ImageJ.

2.8 RNA isolation, cDNA and qRT-PCR

RNA isolation was carried out for cells cultured in BME and microfluidic chips using NucleoSpin RNA Mini kit (Macherey Nagel) according to manufacturer's instruction. RNA was isolated from cells cultured in scaffolds using Qiazol Lysis reagent and RNeasy mini kit (Qiagen). The Nanodrop 2000 (Thermo Fisher) was used to quantify the amount of RNA. 200ng RNA was reverse transcribed to synthesize cDNA using PrimeScript™ RT-PCR Kit (Takara). cDNA was amplified with SYBR™ Green PCR Master Mix (Applied Biosystems™) and specific primers which can be found supplemental Table 9. The mRNA expression levels were measured using the Applied Biosystems 7500 Real-Time PCR system.

2.9 Statistics

The relative mRNA expression levels were determined by the delta CT method and normalized to the geomean of the housekeeping genes GAPDH and HPRT. GraphPad Prism software version 8 (GraphPad Software, La Jolla, CA, USA) was used to analyze the obtained data. A two-tailed unpaired Mann-Whitney U was used to determine the significance between two data groups of the scaffold experiment. P-values of $p \leq 0.05$ were considered significant.

3 RESULTS

CCA organoids isolated from CCA patients' tissue were used to develop an *in vitro* organoid-based EMT model. EMT activation was examined by using different aspects of the tumor microenvironment. Important factors of interest, such as growth factors, ECM and fluid flow, could stimulate the activation of EMT in CCA organoids.

3.1 Effect of various growth factors on EMT activation

Previous studies have demonstrated that growth factors, such as TGF-β1, TNF-α and/or Il-6, could induce EMT in epithelial cell lines. Therefore, we investigated whether these growth factors could also mediate EMT in CCA organoids. CCA organoids derived from CCA patients were cultured in BME with EM^- as shown in Figure 4. CCA organoids have a round shape consisting of a single layered epithelium. However, the epithelium layer of CCA27 looks thicker and includes some irregularities in the organoid shape as indicated in Figure 4. CCA1 originated from pCCA, while CCA14 and CCA27 originated from iCCA. The genomic profile of CCA organoids can be found in supplemental Table 5.

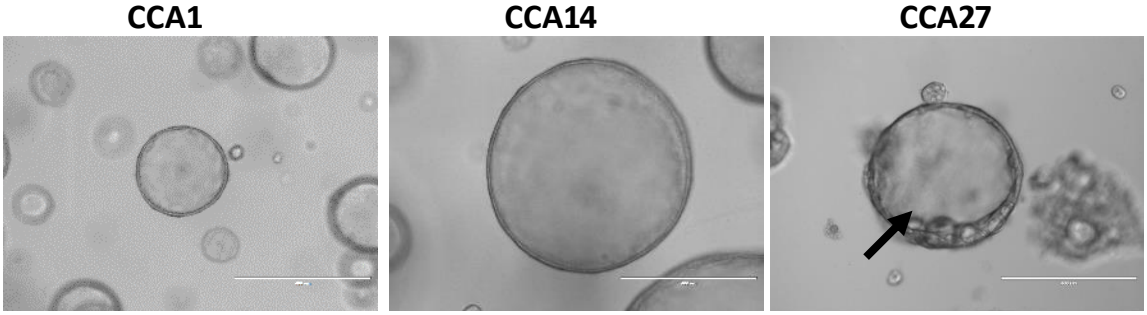

Figure 4: CCA organoids cultured in BME with EM^-. CCA organoids were derived from different patients (n=3). CCA organoids adopt a round shape of single layered epithelium. The arrow highlights the irregularities in the organoid shape of CCA27 (scale bar is 400µm). The genomic profile of CCA organoids can be found in supplemental Table 5.

To explore the effects of TGF-β1, TNF-α and Il-6 in CCA organoids, different concentrations and combinations of these growth factors were added to the culture medium one day after initial seeding of CCA organoids (Figure 5A). The phase-contrast image of CCA organoids cultured under different growth factor conditions for 7 days are shown in Figure 5B. No significant morphological differences were observed between the control and various growth factor conditions. Additionally, the components of cell nucleus and cytoplasm were visualized using H&E staining which did not result in significant morphological changes between the conditions (Figure 5C).

Furthermore, qRT-PCR data was obtained for relative mRNA expression of proliferation marker, Ki67, and various EMT markers including epithelial markers (E-cadherin, KRT19) and mesenchymal markers (Vimentin, Fibronectin, SNAI1) (Figure 6). The qRT-PCR data showed slight differences in the relative mRNA expression of EMT markers in CCA1 and CCA14. In comparison with the control condition of CCA1, vimentin mRNA expression level was increased by ~1.5 fold after combined treatment of 20ng/ml TNF-α and 2ng/ml TGF-β1. Fibronectin mRNA expression level was also increased by ~5 fold after 20ng/ml TGF-β1 treatment. For CCA14, SNAI1 mRNA expression was increased by ~2.5 fold. However, increased mRNA expression levels of mesenchymal markers were not detected for CCA27 and therefore not included in the following experiments. Based on this qPCR analysis, several conditions were selected for the next experiments to further optimize the activation of EMT in CCA.

3.2 Effect of different culture media on EMT activation

The culture conditions of CCA organoids could influence and stimulate EMT. Therefore, CCA organoids were cultured in three different medium compositions including expansion medium (EM), tumor differentiation medium (TDM) and branching medium (BM) (Figure 7A). To examine whether the culture medium could mediate TGF-β1 in EMT activation, 20ng/ml TGF-β1 was added to the different culture media for 7 days. Figure 7B shows phase-contrast images CCA organoids cultured under different culture conditions. CCA1 organoids in EM formed a single layer of epithelial cells which surrounds a central lumen, while CCA organoids in TDM formed smaller and denser structures. CCA1 organoids in BM alternately grew in single layered epithelium structures or denser branching structures which correspond to the native tumor. However, we did not observe significant differences in morphology between the culture conditions treated with and without 20ng/ml TGF-β1. Similar organoid structures were observed for CCA14 organoids. Additionally, qRT-PCR data was analyzed for E-cadherin, KRT19, vimentin, fibronectin, SNAI1 and Ki67. In comparison with EM^- and TDM, CCA organoids cultured in BM resulted in the most substantial difference in expression of EMT markers after TGF-β1 treatment. E-cadherin expression was relatively similar for CCA organoids treated with and without TGF-β1 in BM, while vimentin, fibronectin and SNAI1 expression were upregulated after TGF-β1 treatment.

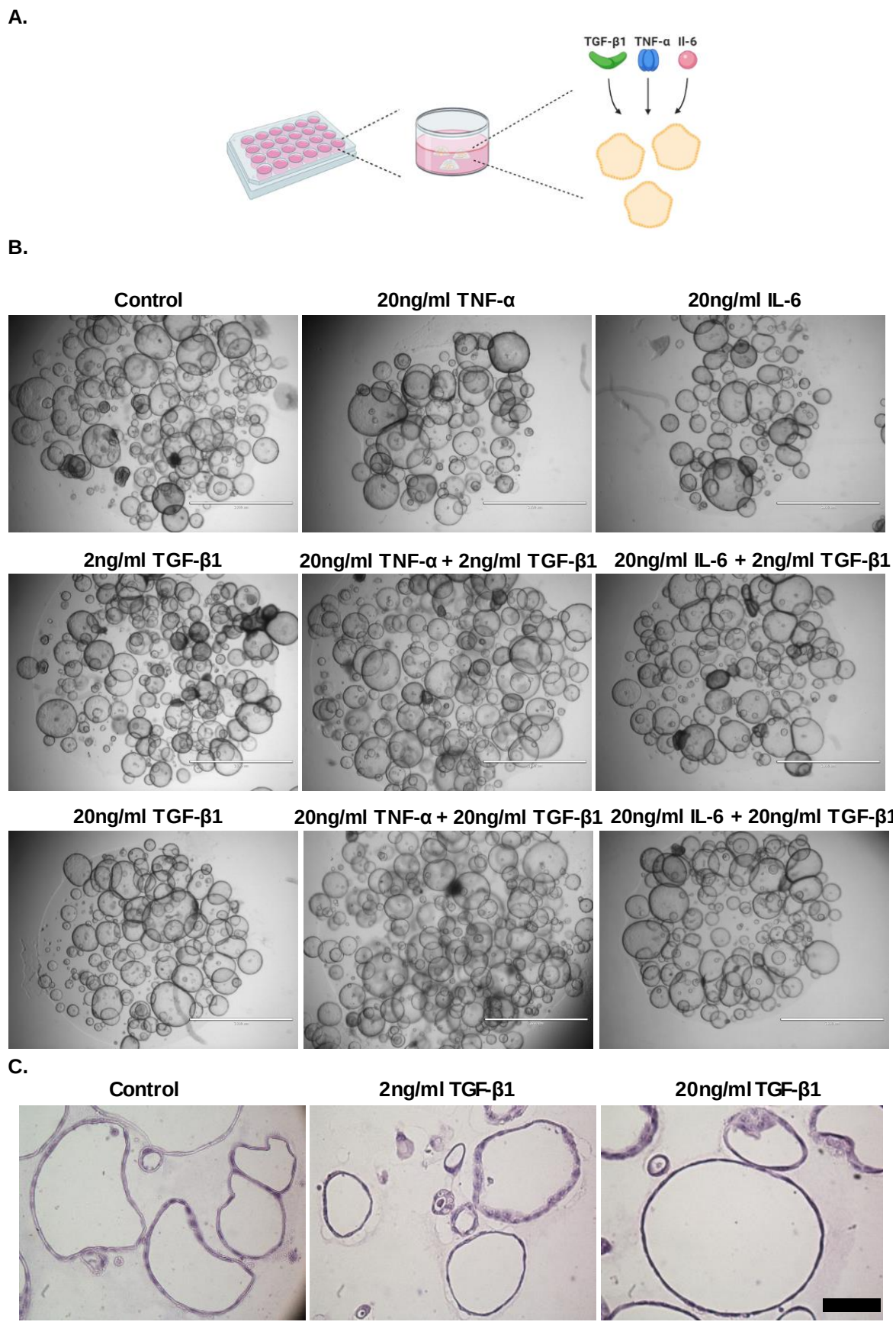

Figure 5: Various growth factor treatments in CCA organoids. A: Schematic overview of CCA organoids treated with different concentrations and combinations of growth factors in BME and EM^{-}. **B:** Phase-contrast images of CCA organoids show no significant morphological differences between the conditions after 7 days (scale bar is 2000µm). **C:** H&E staining of CCA organoids also resulted in similar morphology between the culture conditions (scale bar is 20µm).

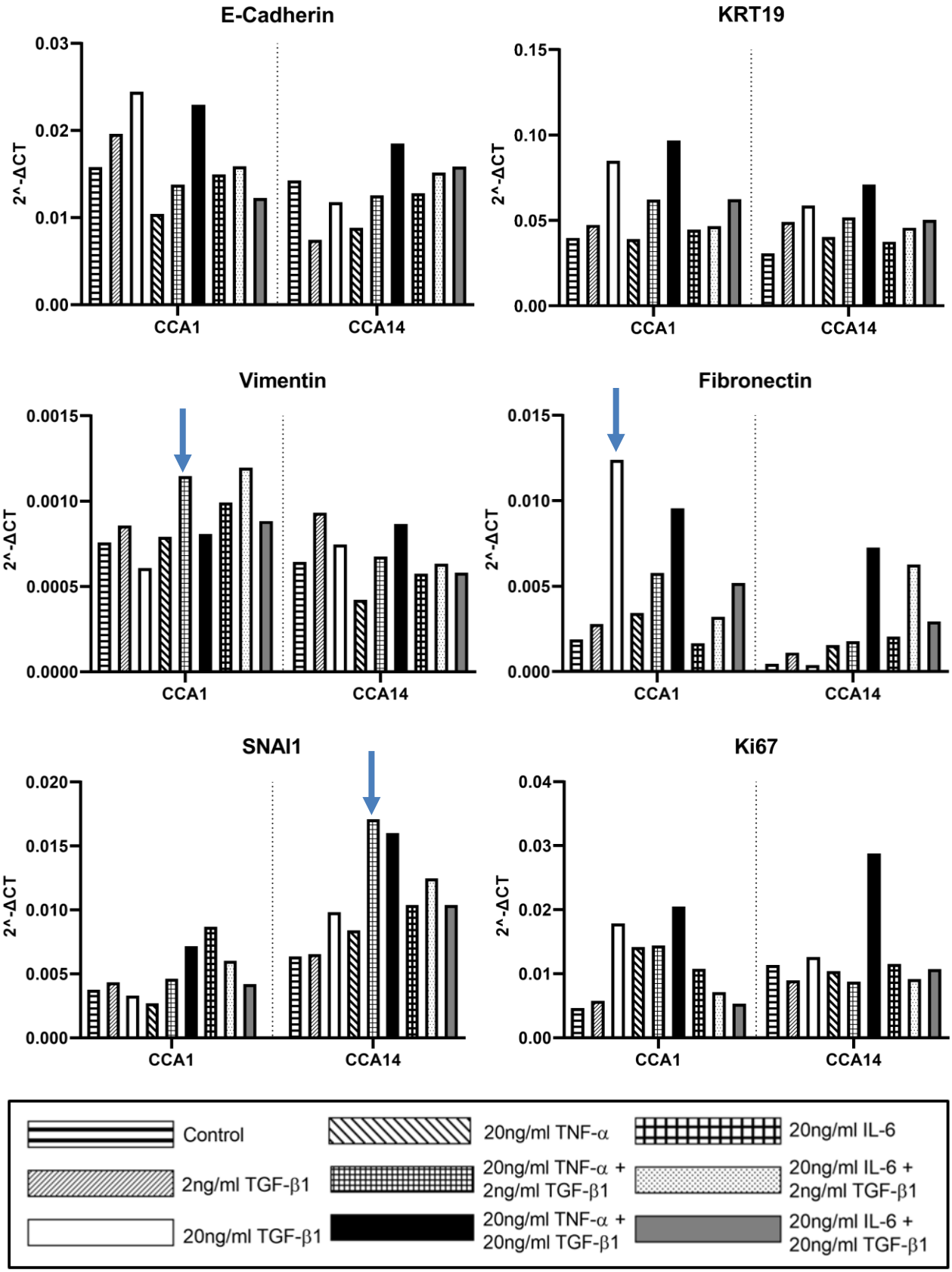

Figure 6: qRT-PCR analysis of CCA organoids cultured in BME and EM$^-$. The graphs show relative mRNA expression levels of epithelial markers (E-cadherin, KRT19), mesenchymal markers (Vimentin, Fibronectin, SNAI1) and proliferation marker (Ki67). These graphs were normalized to GAPDH. The arrows (blue) highlight the upregulation of mesenchymal markers for specific growth factor treatments.

A.

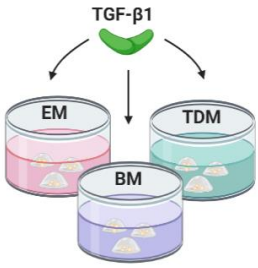

B.

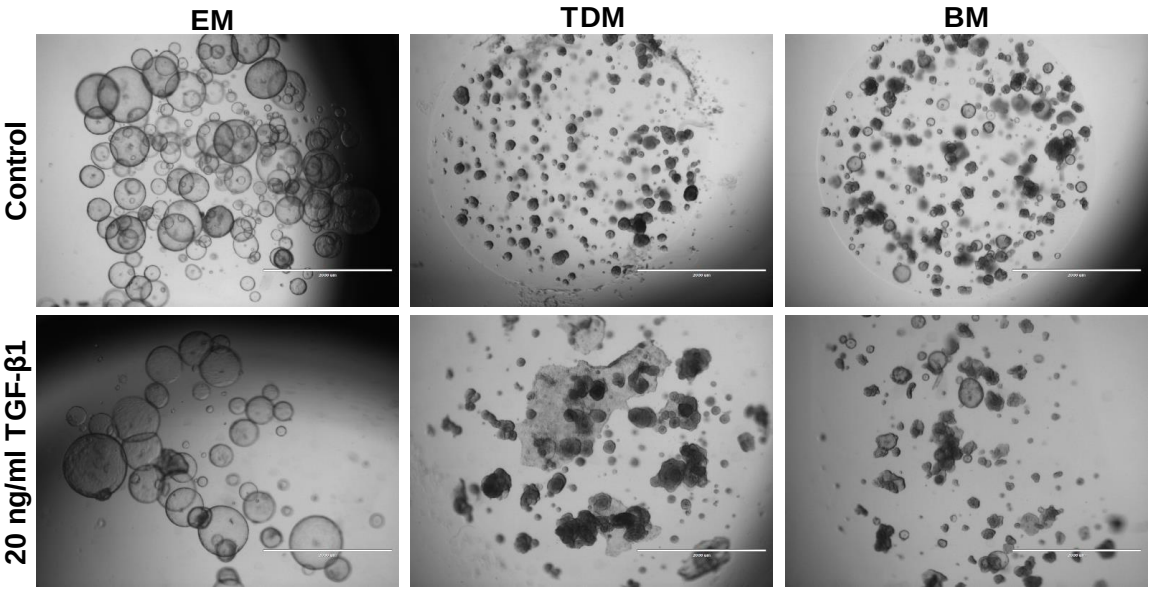

Figure 7: CCA organoids cultured in different medium compositions. A: Schematic representation of CCA organoids cultured in expansion medium without A8301 (EM^-), tumor differentiation medium (TDM) and branching medium (BM). **B:** Phase-contrast images of CCA organoids show morphological differences between the culture media, but no morphological differences were observed between the control and TGF-β1 treatment (scale bar is 2000µm).

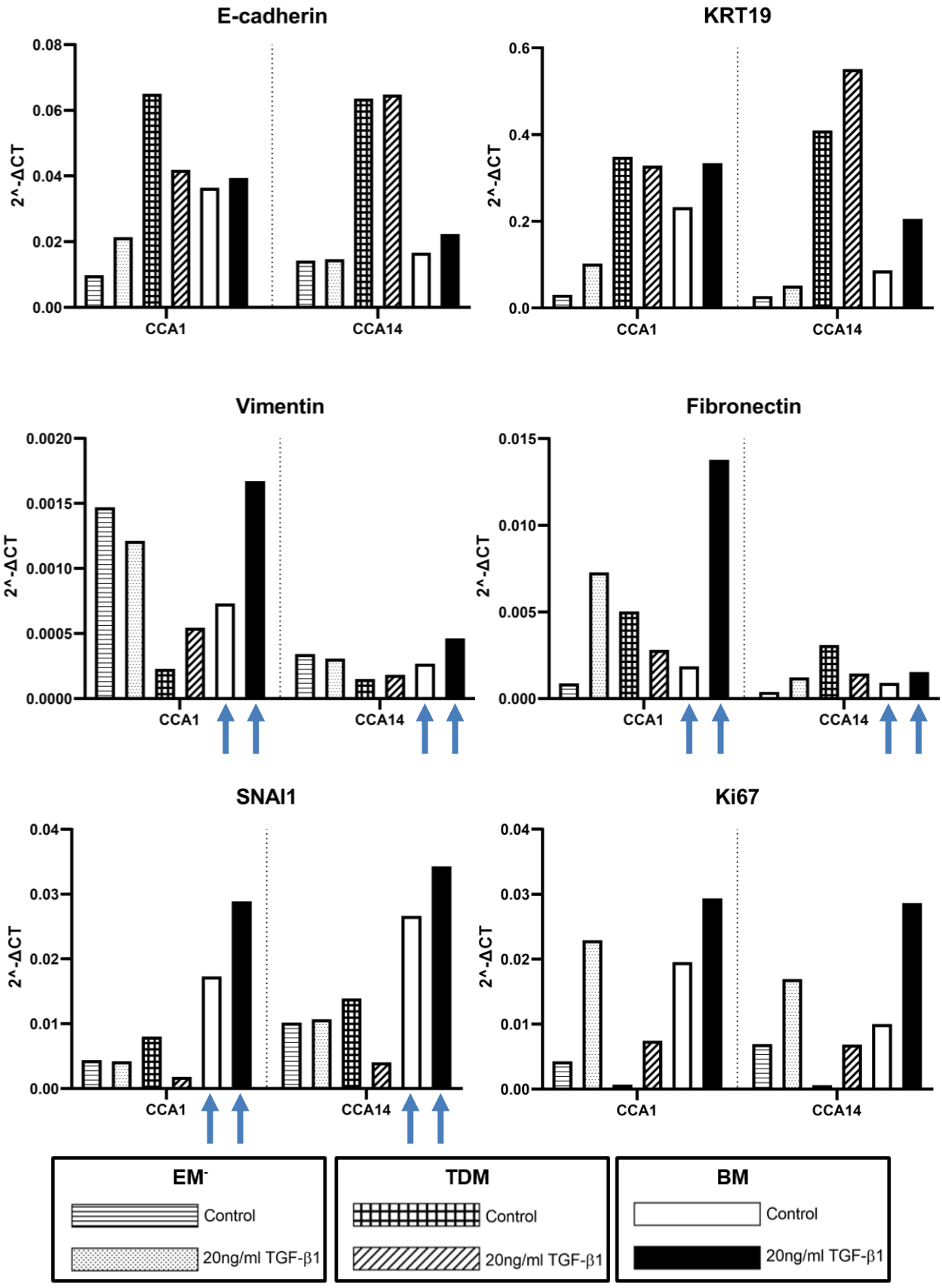

Figure 8: qRT-PCR analysis of CCA organoids cultured in BME and different culture media. The graphs show relative mRNA expression levels of epithelial markers (E-cadherin, KRT19), mesenchymal markers (Vimentin, Fibronectin, SNAI1) and proliferation marker (Ki67). These graphs were normalized to GAPDH. Compared to expansion medium without A8301 (EM^-) and tumor differentiation medium (TDM), the most substantial increase in mRNA expression of mesenchymal markers was observed in branching medium (BM) after TGF-β1 treatment (blue arrows).

3.3 Optimized culture conditions to induce EMT in CCA organoids

Based on the previous results, the culture conditions were optimized for activation of EMT in CCA organoids. BM was combined with 2ng/ml TGF-β1, 20ng/ml TGF-β1, 20ng/ml TNF-α + 2ng/ml TGF-β1 or 20ng/ml IL-6 + 2ng/ml TGF-β1 treatment. As a result, a mixed morphology of single layered epithelium structures (Figure 10, arrow 1) and branching structures (Figure 10, arrow 2) were observed. However, 20ng/ml TNF-α + 2ng/ml TGF-β1 treatment resulted in a higher ratio single layered epithelium structures than branching organoids compared to the control condition. H&E staining of CCA organoids in BM showed more dense structures compared to EM, but there were no significant morphological differences between growth factor treatments in BM (Figure 9). qRT-PCR analysis resulted in a reduced E-cadherin expression and an increased expression of vimentin, fibronectin, ZEB1 and MUC1 after 20ng/ml TGF-β1 or 20ng/ml TNF-α + 2ng/ml TGF-β1 treatment. The relative mRNA expression levels of cancer-associated fibroblasts (CAFs) were also included as positive control (Figure 11). E-cadherin was not detected in CAFs, while mesenchymal markers showed significant higher expression in CAFs than in CCA organoids.

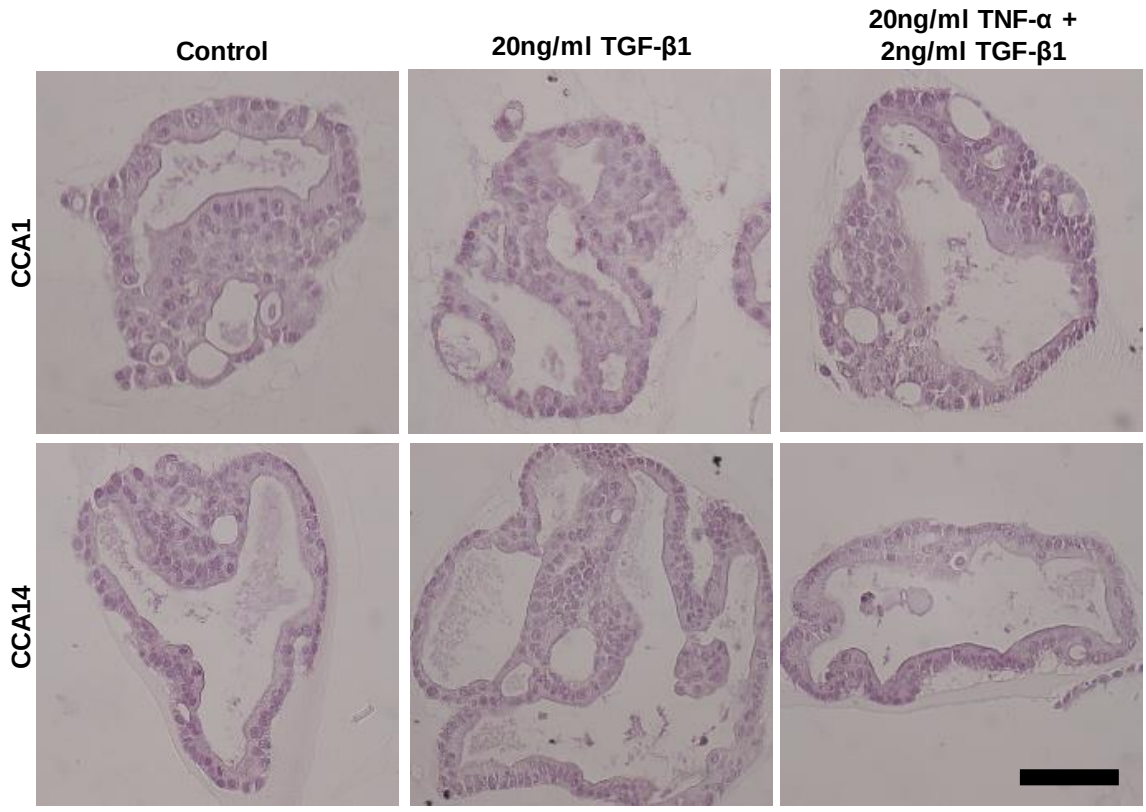

Figure 9: H&E staining of CCA1 and CCA14 organoids after TGF-β1 and TNF-α treatment in BM for 7 days. CCA organoids adopted a branching structure for all growth factor conditions (Scale bar is 20µm).

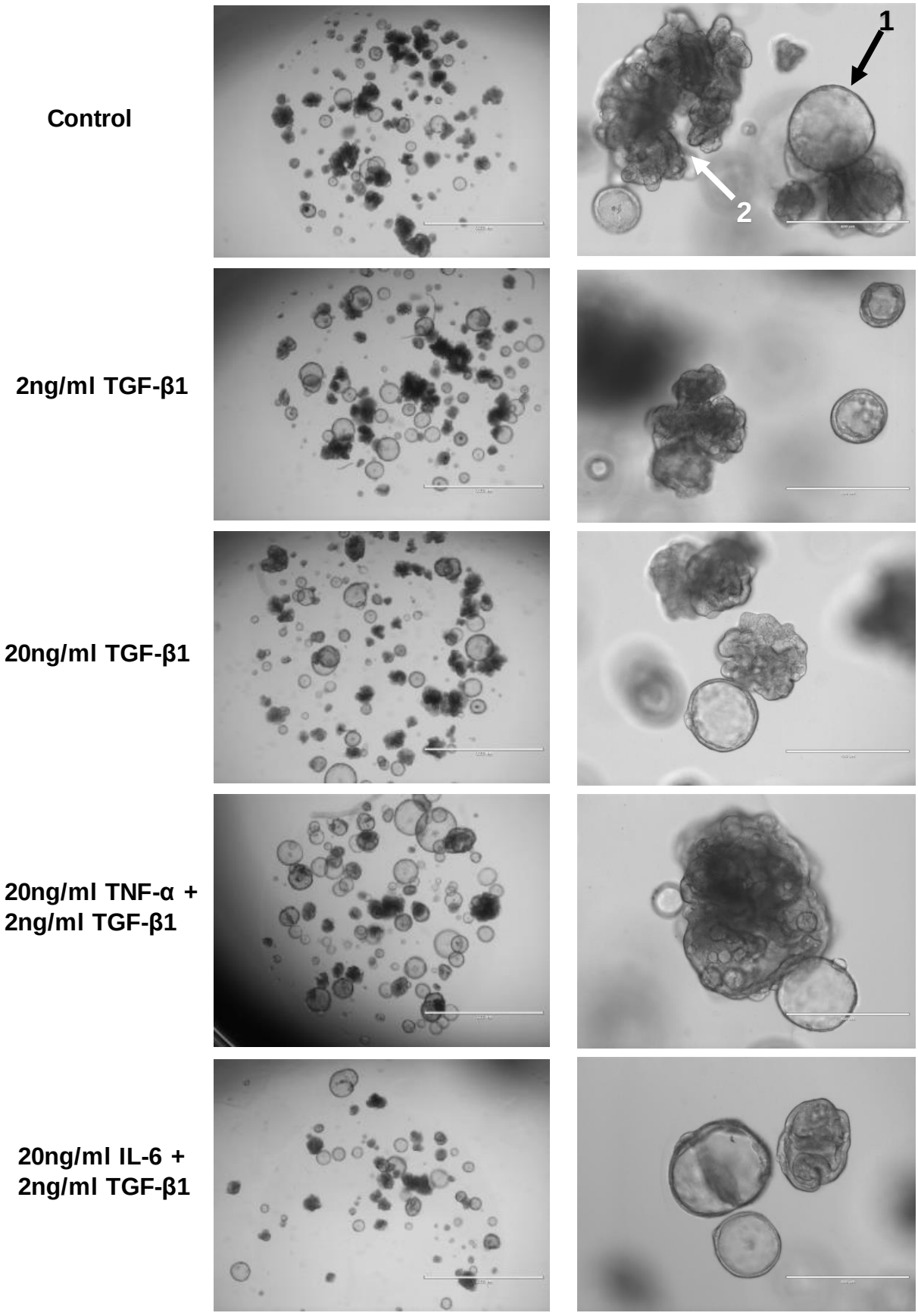

Figure 10: Phase-contrast images of CCA organoids treated with different concentrations of TGF-β1, TNF-α and IL-6 in BME with BM for 7 days. CCA organoids showed a mixed morphology of single layered epithelium structures (arrow 1) and branching structures (arrow 2) for all growth factor conditions. (Left scale bar is 2000µm and right scale bar is 400µm).

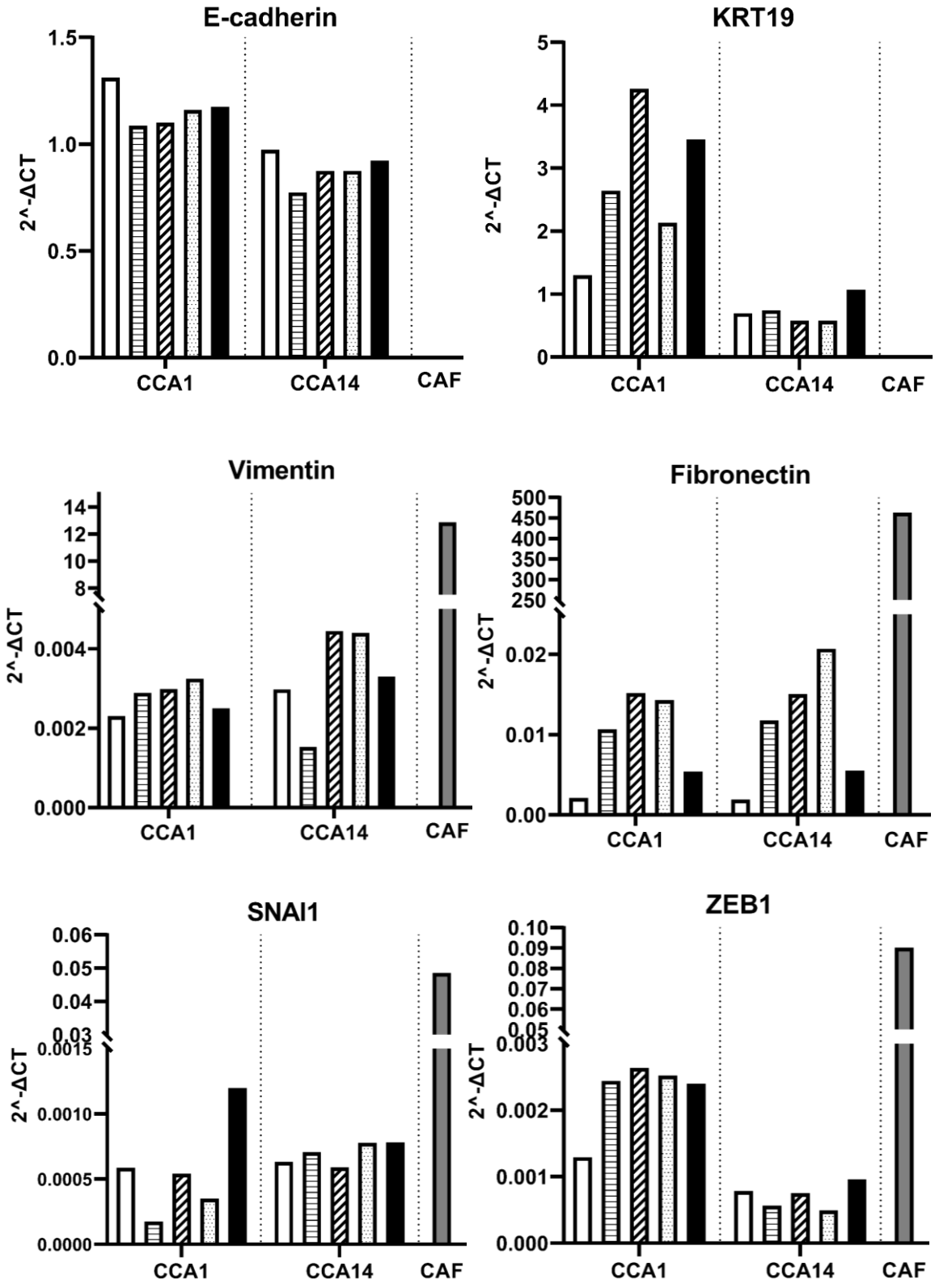
E-cadherin
2^-ΔCT
1.5
1.0
0.5
0.0
CCA1
CCA14
CAF
KRT19
2^-ΔCT
5
4
3
2
1
0
CCA1
CCA14
CAF
Vimentin
2^-ΔCT
14
12
10
8
0.004
0.002
0.000
CCA1
CCA14
CAF
Fibronectin
2^-ΔCT
500
450
400
350
300
250
0.02
0.01
0.00
CCA1
CCA14
CAF
SNAI1
2^-ΔCT
0.06
0.05
0.04
0.03
0.0015
0.0010
0.0005
0.0000
CCA1
CCA14
CAF
ZEB1
2^-ΔCT
0.10
0.09
0.08
0.07
0.06
0.05
0.003
0.002
0.001
0.000
CCA1
CCA14
CAF

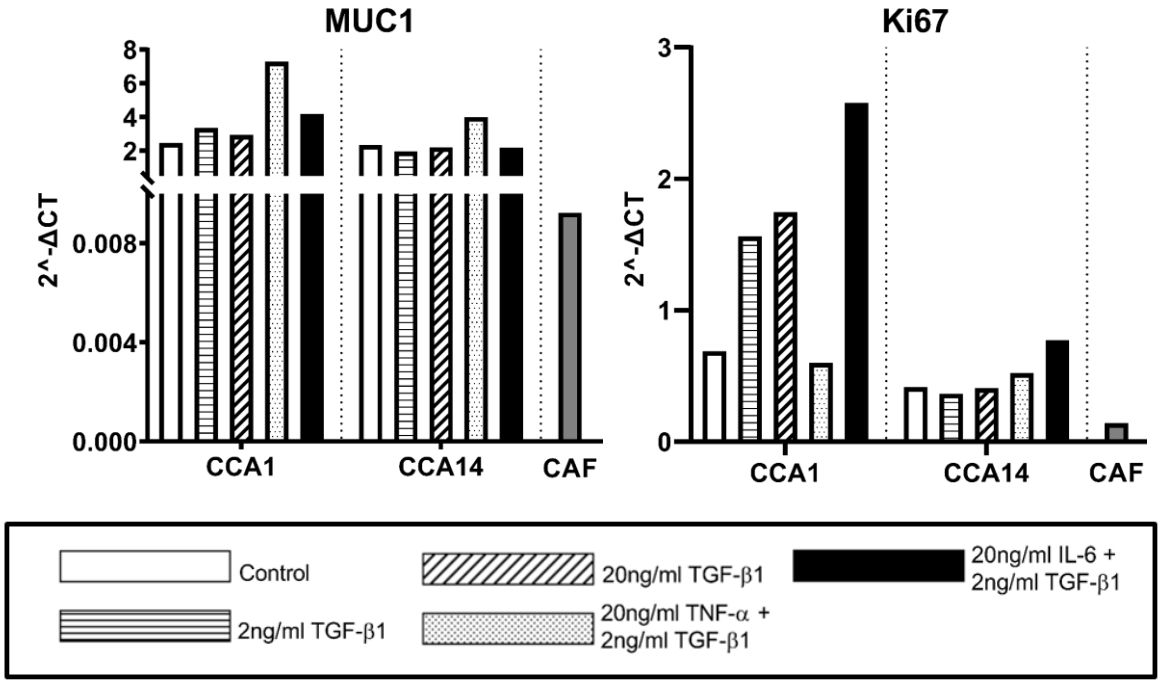

Figure 11: qRT-PCR analysis of CCA organoids cultured in BME with BM. The graphs show relative mRNA expression levels of epithelial markers (E-cadherin, KRT19), mesenchymal markers (Vimentin, Fibronectin, SNAI1, Zeb1, Muc1) and proliferation marker (Ki67). The mRNA expression levels of cancer-associated fibroblasts were included as a positive control. These graphs were normalized to GAPDH and HPRT.

3.4 Effect of extracellular matrix on EMT activation

Besides various growth factors, the ECM is a crucial aspect of the tumor microenvironment. To investigate the effect of ECM on EMT induction in CCA, donor and tumor ECM were obtained using decellularization process. Cellular material was removed from the ECM scaffold, reseeded with CCA organoids and treated with TGF-β1 and TNF-α as shown in Figure 12A. Figure 12B shows an example of a tissue punch before and after decellularization. The decellularized tissue punch was cut into slices with a thickness of 200µm and reseeded with CCA organoids. Phase-contrast images of donor and tumor ECM scaffolds seeded with CCA organoids are shown in Figure 12C. All ECM scaffolds possessed their own unique structure. Macroscopically, donor ECM scaffold were stickier and contained more fat, while tumor ECM scaffold consisted of denser and stiffer structures. After 14 days in culture, tumor and donor scaffolds with cells were cut into sections of 4µm and stained with H&E to examine the ingrowth of cells into the scaffolds. Figure 13 displays three H&E sections (top, middle and bottom) of a tumor and donor scaffold including the TGF-β1 condition. CCA organoids did mainly grow on top and at edges of the scaffold for all culture conditions. H&E sections of the complete scaffolds can be found in supplemental Figure 25-Figure 28. Close-up H&E scaffold images showed that CCA organoids formed denser structures along the ECM in donor scaffolds, while these cells were less attached to each other in the tumor scaffolds(Figure 14). After TGF-β1 treatment, cells formed gaps in tumor as well as donor scaffolds. Specifically in tumor scaffolds, cells adopt a more stretched morphology (Figure 14).

To further analyze the morphology of cells after TGF-β1 treatment in different ECM scaffolds, nuclear components of the cell were stained with DAPI and F-actin filaments with Phalloidin. Supplemental Figure 30 shows that CCA organoids did grow in alignment with the ECM surface and were attached to the scaffolds. Cells adopted an epithelial-like morphology with a polygonal cell shape and regular cell nucleus dimensions in both tumor (Figure 15) and donor (Figure 16) scaffolds. The epithelial-like cell morphology was also observed in CCA organoids cultured in BME as a control for the staining (supplemental Figure 29). Some cells in the ECM scaffold also showed irregularity in their cell shape, but after addition of TGF-β1 roughly all cells showed irregularity in their cell shape and nucleus dimensions. These cells adopted a more mesenchymal-like structure without a well-defined cell structure. Furthermore, vimentin staining showed vimentin was concentrated at the cell nucleus in the tumor scaffold treated with TGF-β1, while vimentin was also detected around the cell nucleus in the donor scaffold (supplemental Figure 31).

The relative mRNA expression levels were analyzed for CCA organoids (n=2) cultured on tumor (n=3) and donor (n=3) ECM scaffolds (supplemental Figure 24). qRT-PCR data was grouped based on scaffold type to examine the effect of tumor and donor ECM scaffolds on EMT activation (Figure 17). All expression levels for tumor scaffolds were lower than donor scaffolds. The proliferation marker, Ki67, decreased in expression for both donor and tumor scaffolds after 20ng/ml TGF-β1 and/or 20ng/ml TNF-α. The epithelial markers, E-cadherin and KRT19, resulted in a slight decrease in expression for tumor scaffolds treated with 20ng/ml TGF-β1. The relative expression levels of mesenchymal markers, vimentin, fibronectin, ZEB1 and MUC1, resulted in an increase in expression after 20ng/ml TGF-β1 and/or 20ng/ml TNF-α. However, a significant difference was only found for fibronectin expression between control and 20ng/ml TGF-β1 + 20ng/ml TNF-α in donor scaffold. The spread of data points of the conditions was large, therefore the qRT-PCR data was analyzed for specific combinations of CCA organoids and ECM scaffolds. The specific combination of tumor CCA1206 scaffold with CCA1 organoids resulted in a decrease in E-cadherin expression, while tumor CCA2017 scaffolds with CCA14 resulted in an increase of E-cadherin (Figure 18). Mesenchymal markers, vimentin and fibronectin, resulted in an increase of expression for both conditions. However, ZEB1 expression only showed an increase in expression for CCA1206 scaffold, while SNAI1 expression was only increased in CCA2017 scaffold. The specific combinations of CCA organoids with ECM scaffolds influenced the expression of EMT markers.

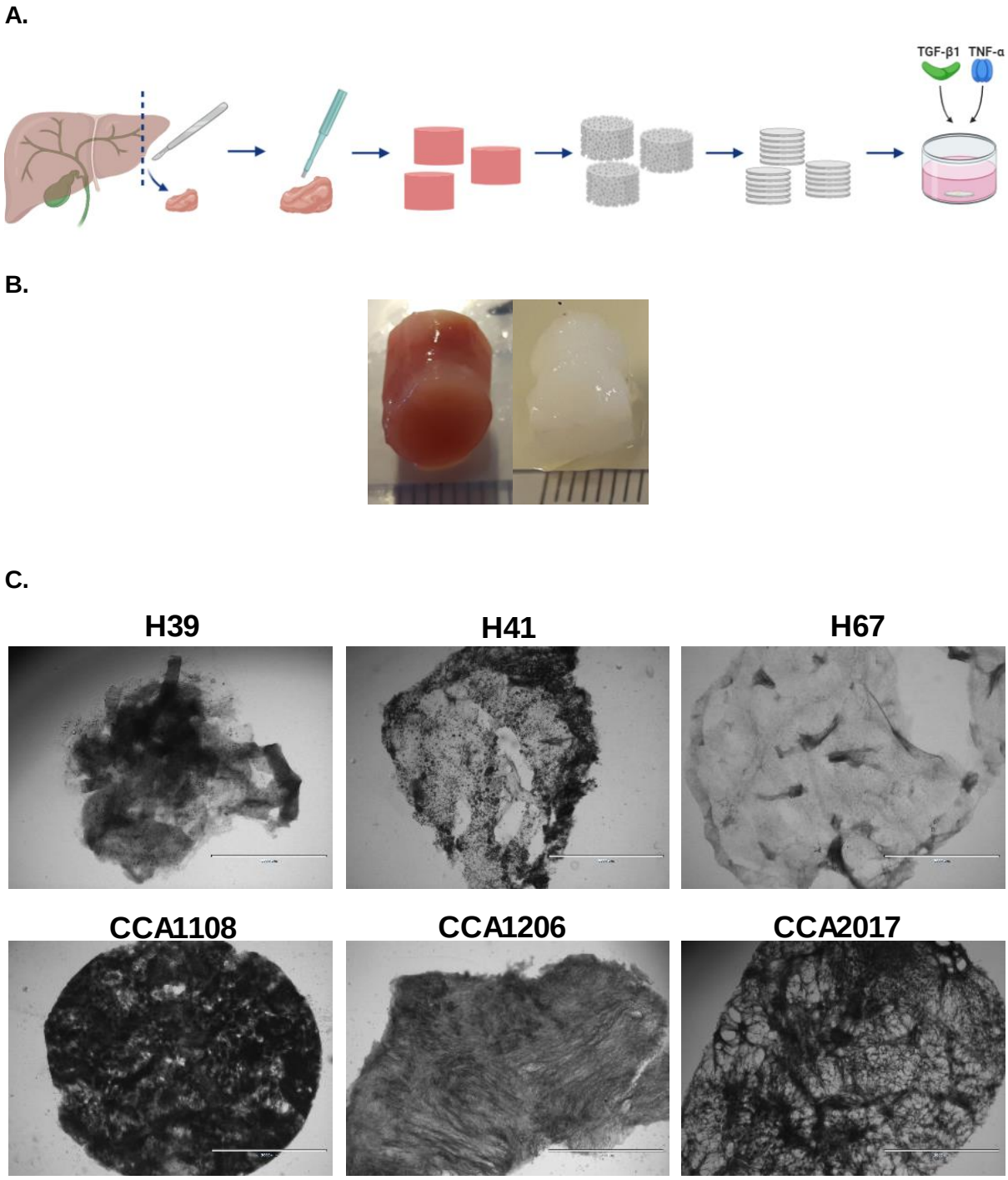

Figure 12: Patient derived extracellular matrix (ECM). A: Schematic overview to obtain scaffold slices. Tissues were obtained by partial resection or rejected donor livers for tumor and donor scaffolds, respectively. Tissue punches of 6mm diameter were obtained using a disposable biopsy punch. The cells were removed from the ECM with the decellularization method. ECM scaffold were cut into slices with a thickness of 200µm. ECM slices were seeded with CCA organoids and treated with TGF-β1 and TNF-α. **B:** Tissue punches before and after decellularization. **C.** Phase-contrast images of donor scaffolds (n=3; H39, H41 and H67) and CCA scaffolds (n=3; CCA1108, CCA1206 and CCA2017) (scale bar is 2000µm).

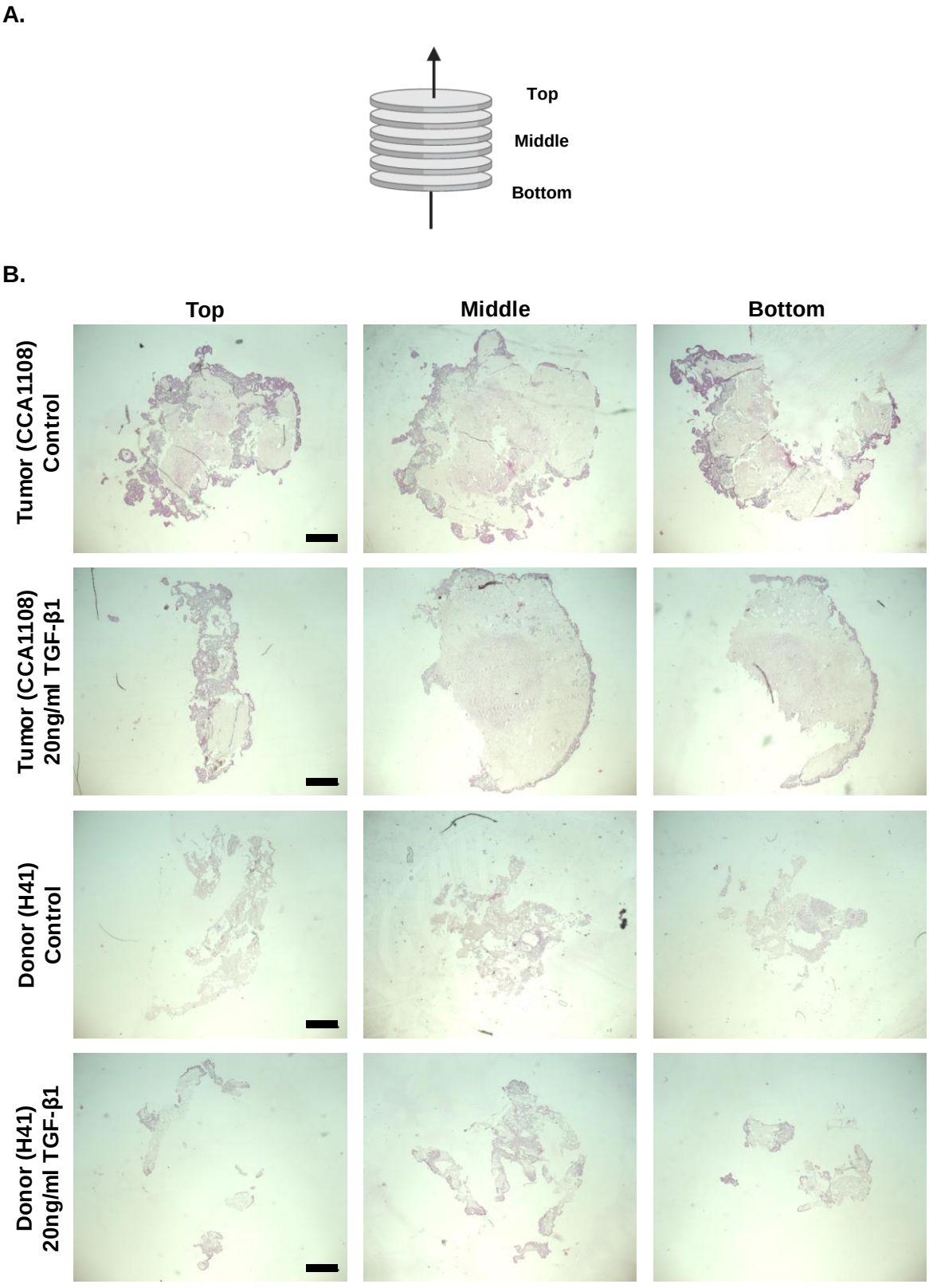

Figure 13: H&E staining of CCA14 organoids cultured on ECM scaffolds with BM. A: The schematic representation of the scaffold displays the position of the sections in the scaffold. **B.** Top, middle and bottom sections of tumor (CCA1108) and donor (H41) scaffolds treated with and without 20ng/ml TGF-β1 (scale bar is 100µm). Cells (purple) were mainly located at on top and at the edges of the scaffolds.

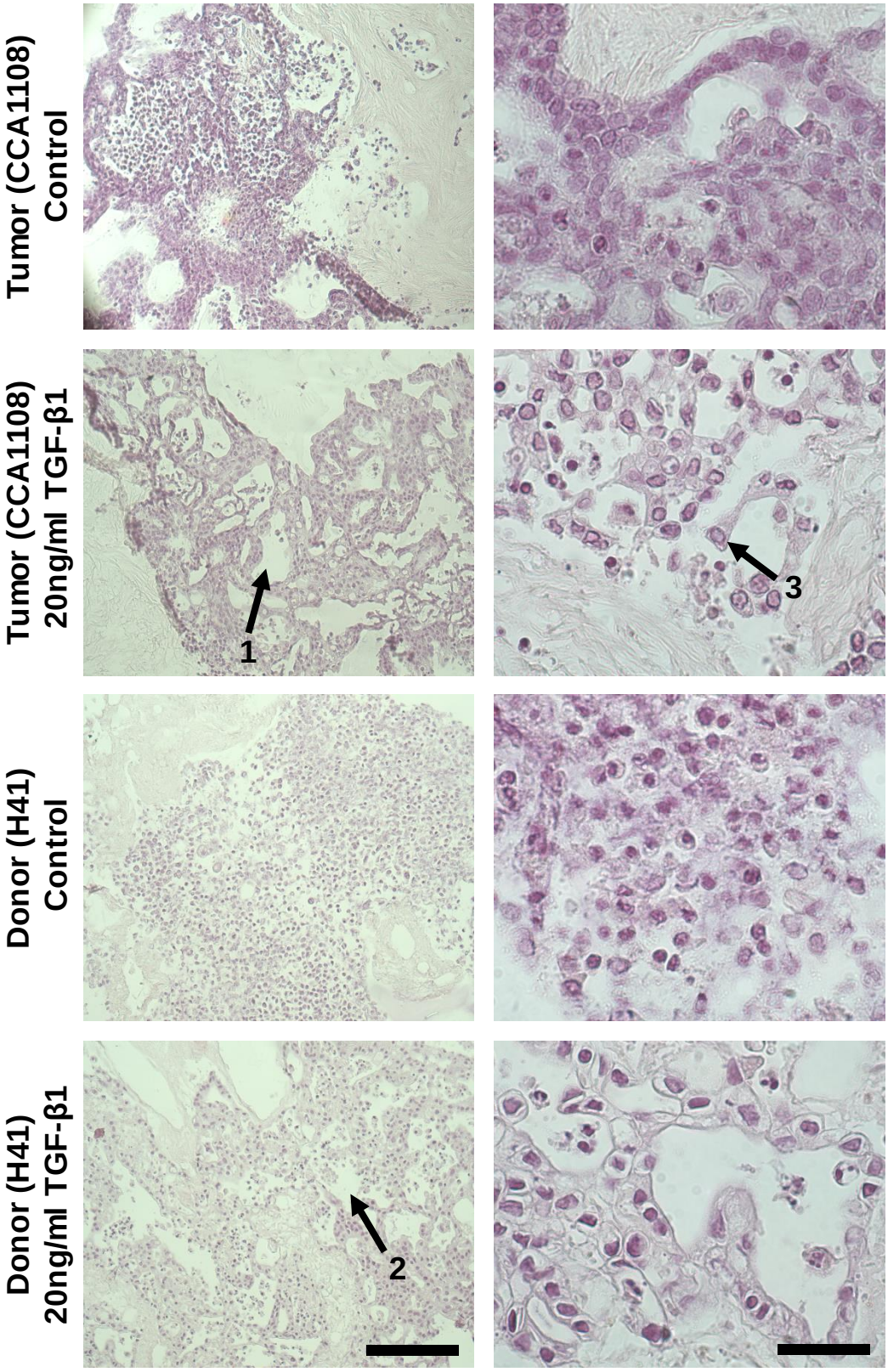

Figure 14: Close up images of H&E staining of CCA14 organoids cultured on ECM scaffolds with BM and TGF-β1. Cells did grow in denser structures in donor scaffold than tumor scaffold. Cells formed gaps in both scaffold types after TGF-β1 treatment (arrow 1&2). Arrow 3 indicates the stretched cell morphology after TGF-β1 treatment in tumor scaffold (scale bar left 50µm and right 10µm).

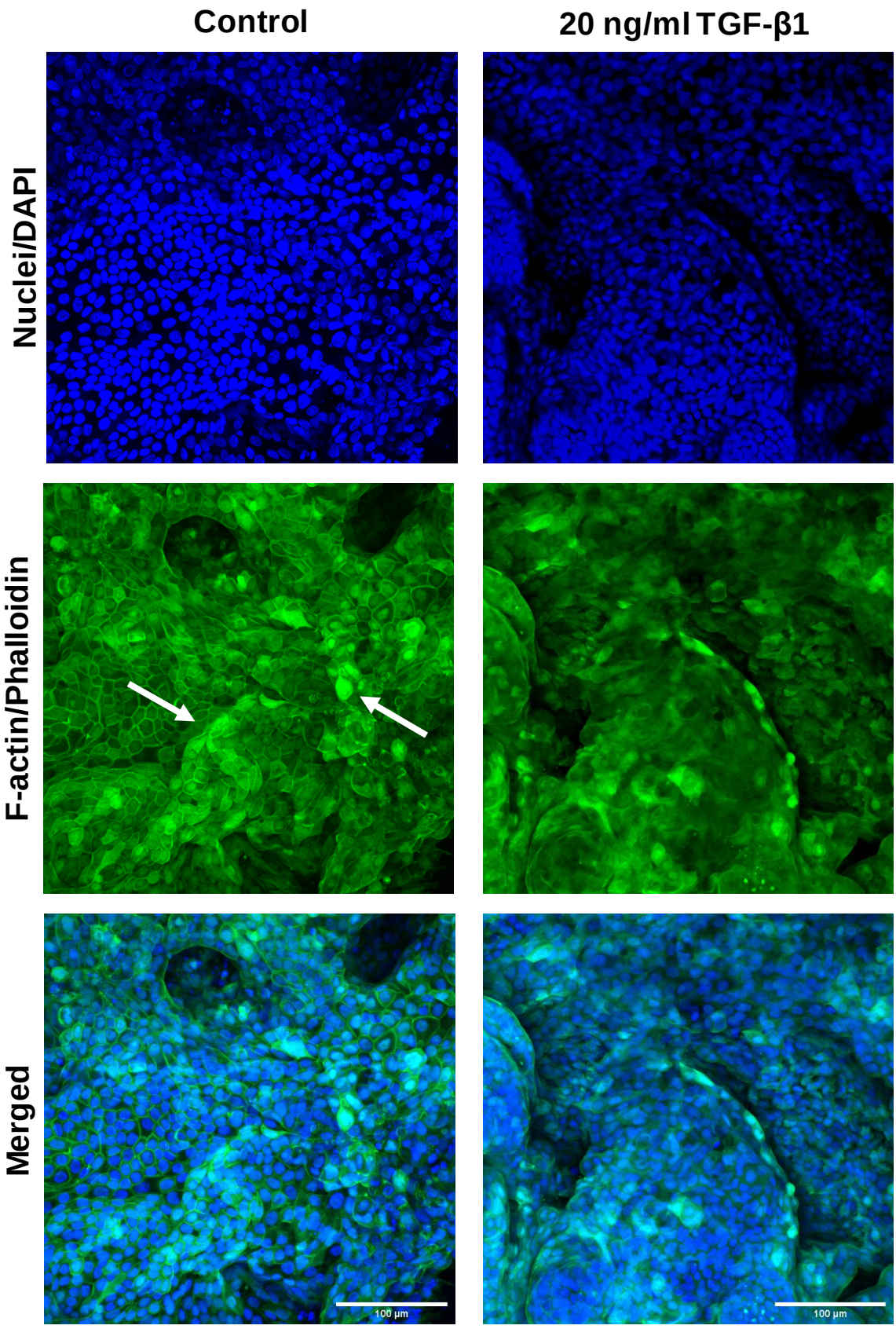

Figure 15: Max intensity projection of CCA14 organoids cultured in tumor (CCA1108) scaffold with BM. Images represent cell nuclei (Blue/DAPI) and F-actin (green/Phalloidin) (scale bar is 100µm). Most cells adopted an epithelial-like morphology for the control condition, but some cells adopted an irregular structure (white arrows). After TGF-β1 treatment, all cells adopted an irregular cell morphology.

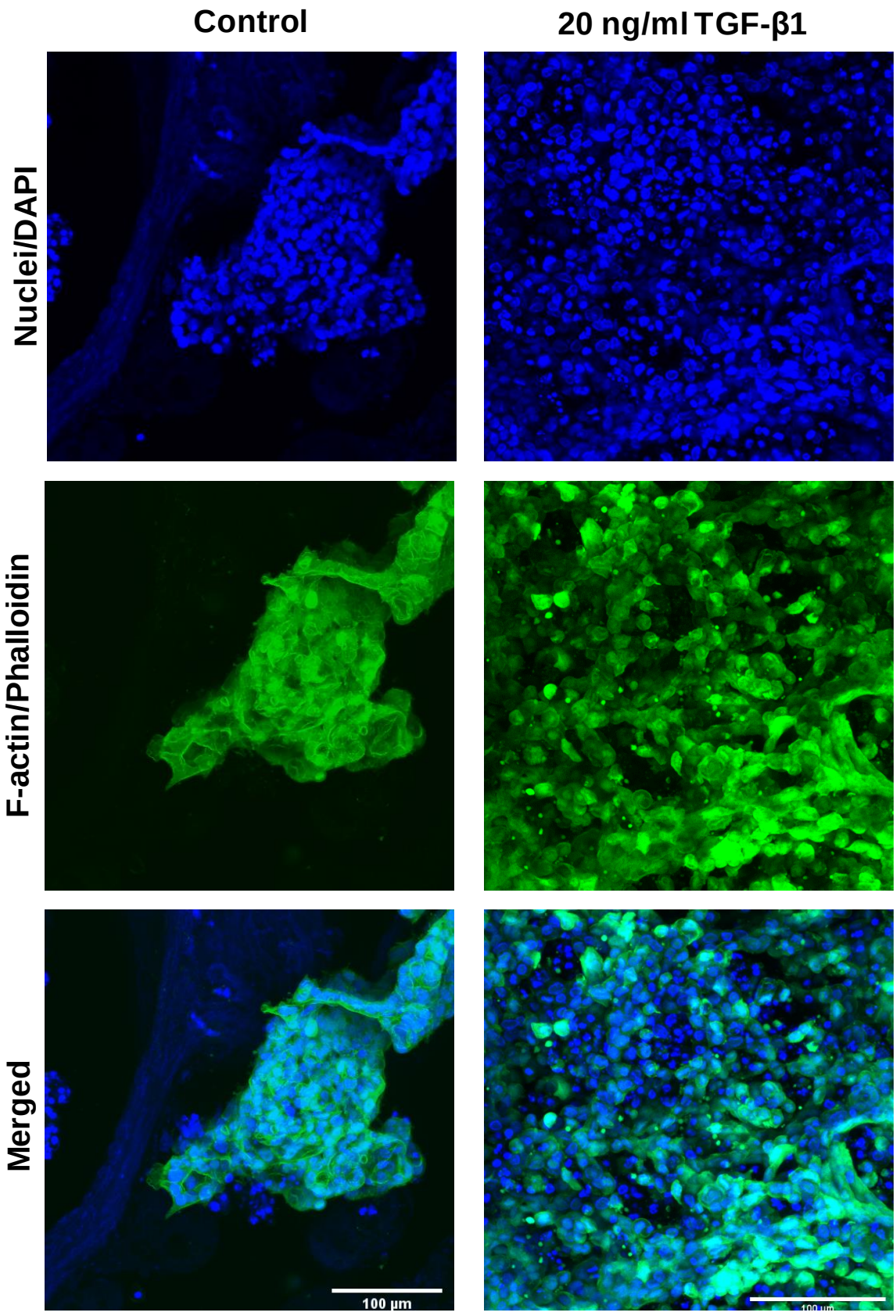

Figure 16: Max intensity projection of CCA14 organoids cultured in donor (H41) scaffold with BM. Images represent cell nuclei (Blue/DAPI) and F-actin (green/Phalloidin) (scale bar is 100µm).

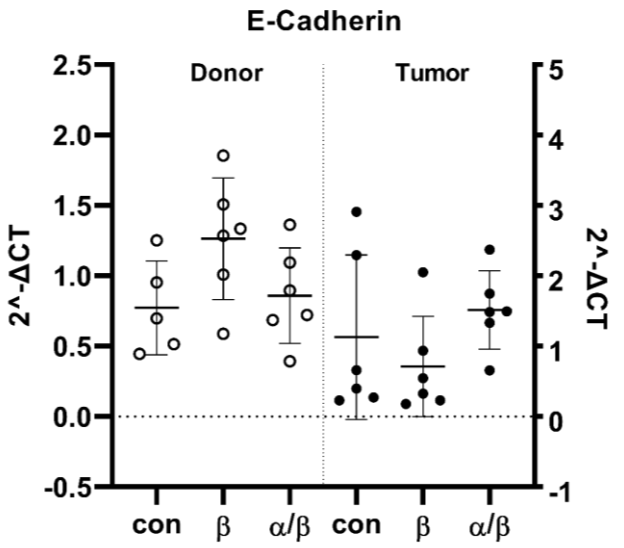
E-Cadherin
Donor
Tumor
2^-ΔCT
2^-ΔCT
2.5
2.0
1.5
1.0
0.5
0.0
-0.5
5
4
3
2
1
0
-1
con
β
α/β
con
β
α/β

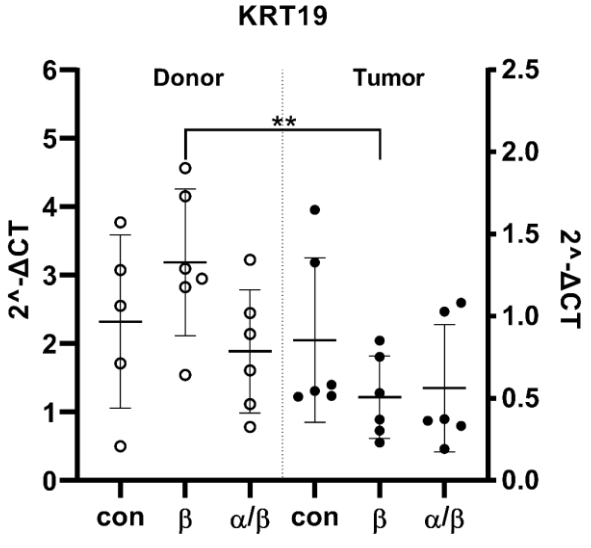
KRT19
Donor
Tumor
**
2^-ΔCT
2^-ΔCT
6
5
4
3
2
1
0
2.5
2.0
1.5
1.0
0.5
0.0
con
β
α/β
con
β
α/β

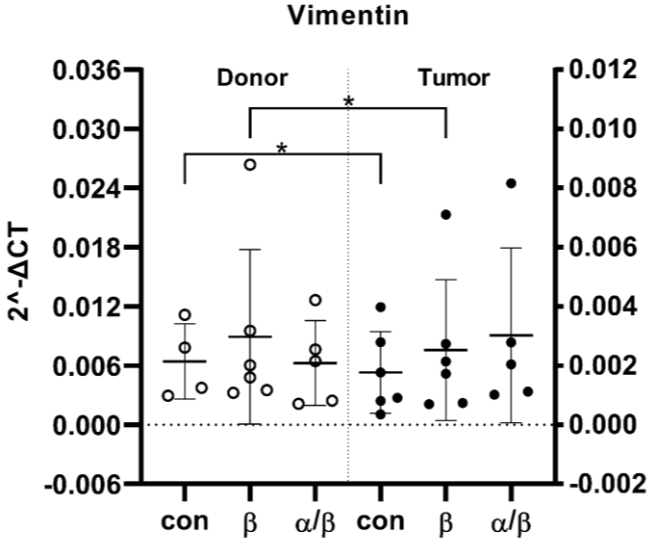
Vimentin
Donor
Tumor
*
*
2^-ΔCT
2^-ΔCT
0.036
0.030
0.024
0.018
0.012
0.006
0.000
-0.006
0.012
0.010
0.008
0.006
0.004
0.002
0.000
-0.002
con
β
α/β
con
β
α/β

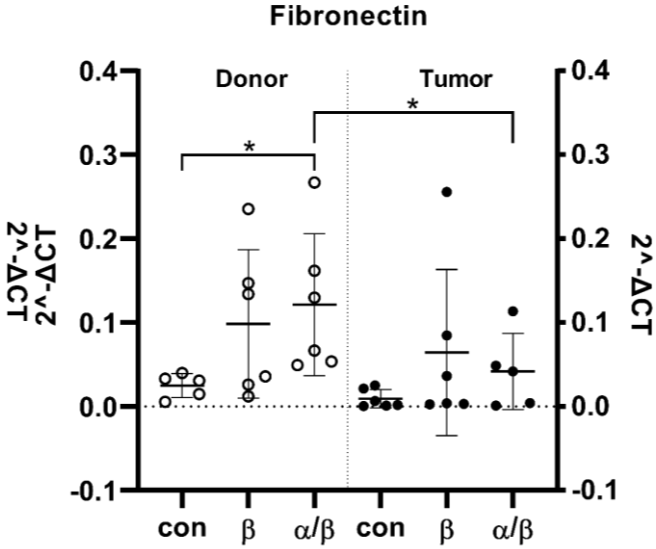
Fibronectin
Donor
Tumor
*
*
2^-ΔCT
2^-ΔCT
0.4
0.3
0.2
0.1
0.0
-0.1
0.4
0.3
0.2
0.1
0.0
-0.1
con
β
α/β
con
β
α/β

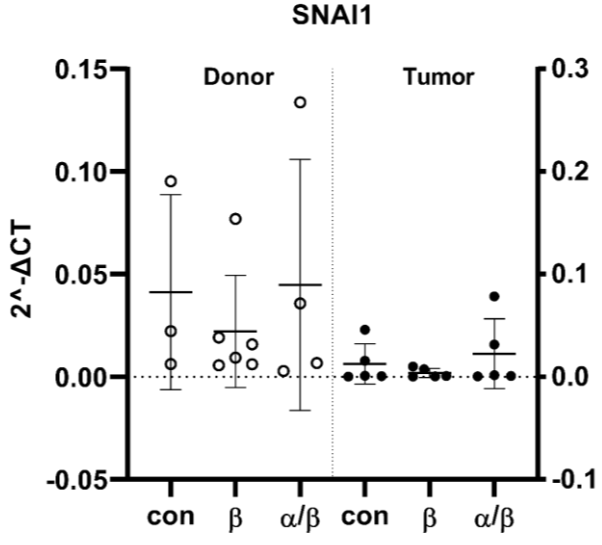
SNAI1
Donor
Tumor
2^-ΔCT
2^-ΔCT
0.15
0.10
0.05
0.00
-0.05
0.3
0.2
0.1
0.0
-0.1
con
β
α/β
con
β
α/β

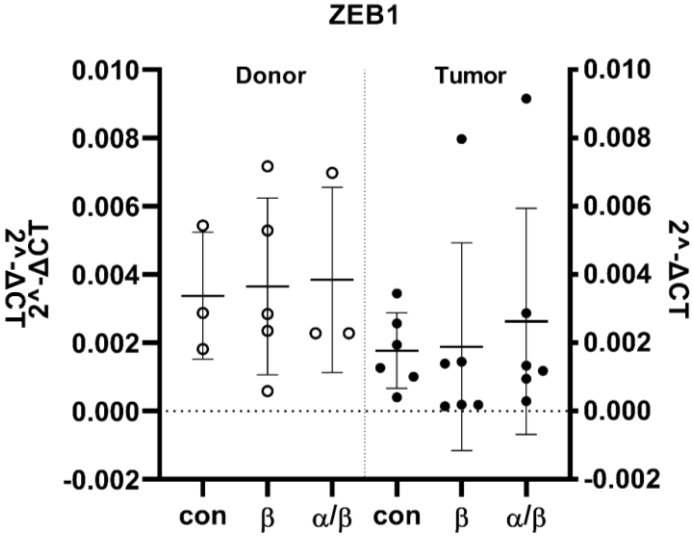
ZEB1
Donor
Tumor
2^-ΔCT
2^-ΔCT
0.010
0.008
0.006
0.004
0.002
0.000
-0.002
0.010
0.008
0.006
0.004
0.002
0.000
-0.002
con
β
α/β
con
β
α/β

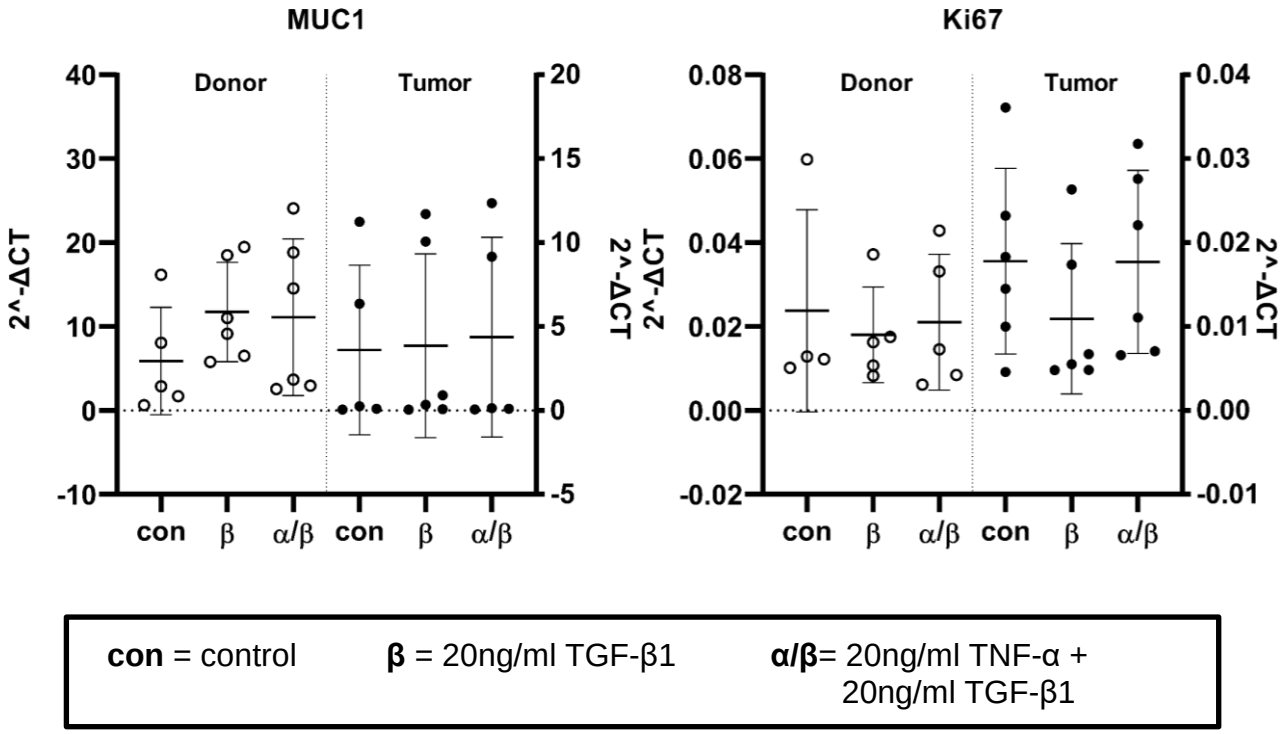

Figure 17: qRT-PCR analysis of CCA organoids cultured on ECM scaffolds with BM. Six different ECM scaffolds (three donor and three CCA scaffolds) and two different CCA organoid types (CCA1 and CCA14) were used. Therefore, the graphs include twelve different conditions which were grouped based on scaffold type (donor or CCA). The graphs show relative mRNA expression levels of epithelial markers (E-cadherin, KRT19), mesenchymal markers (Vimentin, Fibronectin, SNAI1, ZEB1, MUC1) and proliferation marker (Ki67). Data were normalized to GAPDH and HPRT and included the mean ± SD with a Mann-Whitney U test (*p<0.05, **p<0.01).

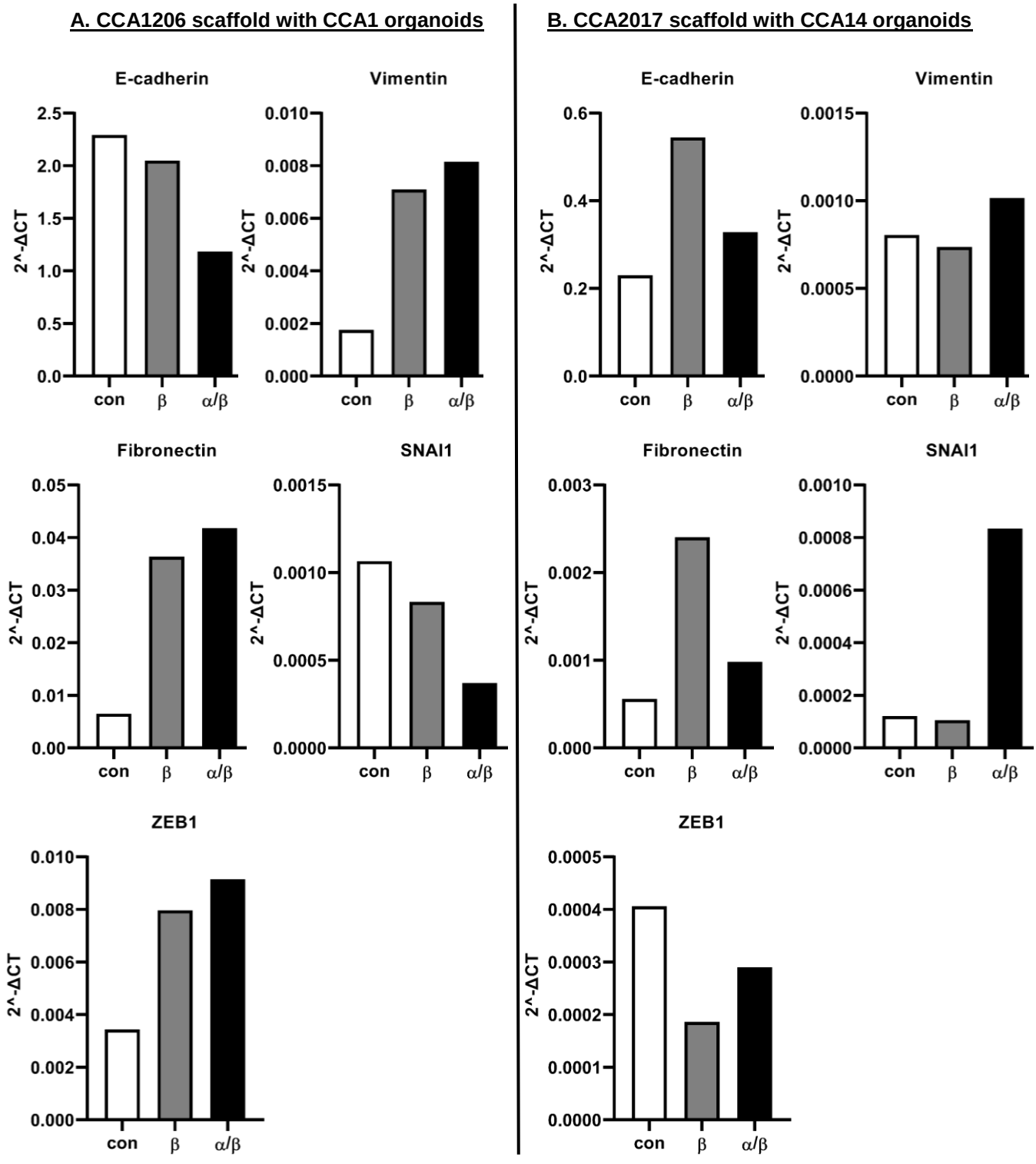

Figure 18: qRT-PCR analysis of specific combinations of CCA organoids cultured on ECM scaffolds with branching medium. The graphs show relative mRNA expression levels of epithelial markers (E-cadherin) and mesenchymal markers (Vimentin, Fibronectin, SNAI1, ZEB1) in **A:** CCA1 organoids cultured in tumor (CCA1206) scaffolds and **B:** CCA14 organoids cultured in tumor (CCA2017) scaffolds.

3.5 Effect of fluid flow on EMT activation

Additionally, the effect of fluid flow on EMT activation was examined by developing a CCA organoids-on-a-chip model. CCA organoids tagged with GFP were cultured on a microfluidic platform (Mimentas) using three different seeding methods (Figure 19). Starting from single cells, organoids were formed in BME for the control condition without a fluid flow (Figure 20). The organoid formation was also observed in the presence of a fluid flow. On top of that, in-gel seeding method with a fluid flow showed that cells migrated into the medium channels after a few days in culture. However, gel-gel seeding method only resulted in organoid formation in the top BME channel after 8 days. Subsequently, some cells migrated and formed organoids in the middle BME channel, but did not migrate further into the bottom medium channel (Supplemental Figure 32). Instead of forming organoid structures, cells seeded with the tubule method did adopt a tube structure in the top medium channel with protrusions growing into the middle BME channel.

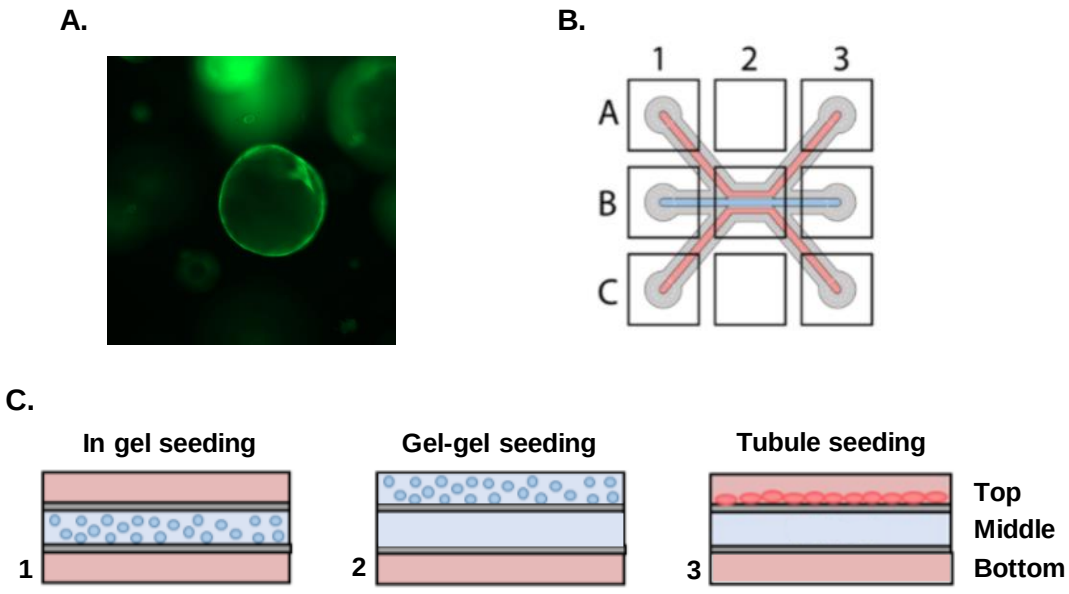

Figure 19: CCA organoids-on-a-chip-model. A: CCA1 organoids tagged with GFP. **B:** Schematic representation of a chip on a 3-lane OrganoPlate Mimetas. 1A, 2A and 3A are the inlets of the channels whereas 3A, 3B and 3C are the outlets of the channels. **C:** Three different methods were used to seed the cells. *1. In gel seeding*: CCA organoids were seeded in the middle channel with BME. The top and bottom channel consist of expansion medium with a flow rate of 121.2µl/h. *2. Gel-gel seeding:* CCA organoids were seeded in the top channel with BME. The middle channel only consists of BME and the bottom channel consists of expansion medium with a flow. *3. Tubule seeding*: CCA organoids were seeded in the top channel in expansion medium with a flow to adopt a tube shape. The middle channel only consists of BME and the bottom channel consists of expansion medium with a flow.

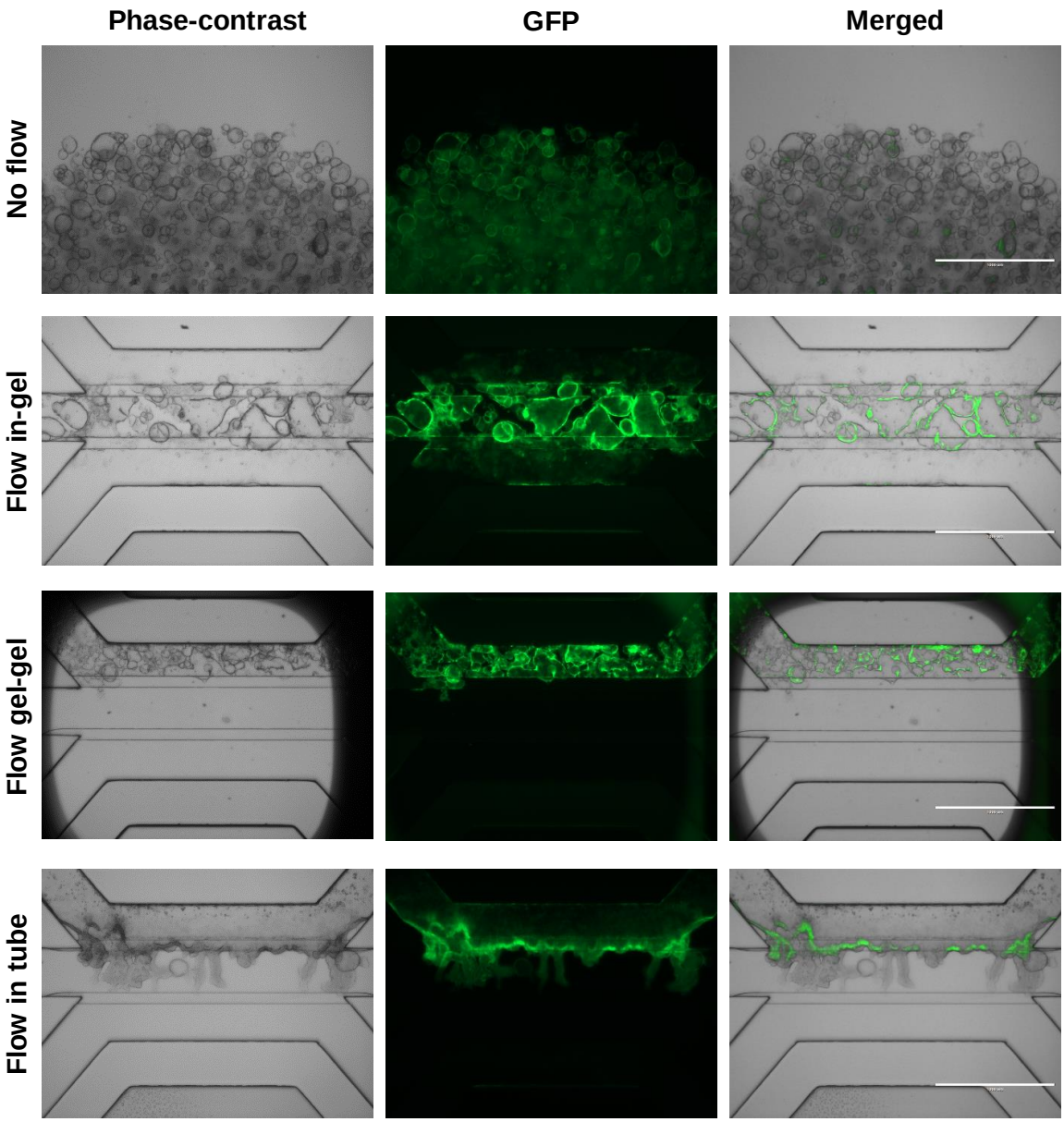

Figure 20: Different culture methods for CCA organoids-on-a-chip. Phase-contrast, GFP and merged images of CCA organoids cultured in the absence and the present of a flow rate for 8 days using different culture methods (scale bar is 1000µm).

To further investigate the effect of the fluid flow on EMT, confocal image were obtained for in-gel and tubule seeding method (Figure 21). The maximum intensity projection images of in-gel seeding confirmed organoid formation in the middle BME channel and migration of cells to the top and bottom medium channels.
To examine whether fluid flow stimulates TGF-β1 in EMT induction, 20ng/ml TGF-β1 was added to the tubule seeding medium. The maximum intensity project images show that cells formed a tube structure in the top channel and protrusions to the middle channel after 8 days for both the control and TGF-β1 condition. However, cells migrated through the middle channel to the bottom medium channel after 5 days of TGF-β1 treatment, while cells without TGF-β1 treatment just started to form protrusions. The tube formation of cells in the top medium channel was confirmed by XYZ-plane images for both conditions (Figure 22A).

3D image analysis showed that cells did grow on top of the BME gel of the middle channel without TGB-β1 treatment, while cells did grow into the BME gel after TGF-β1 treatment. These cells migrate to the bottom channel and formed another tube structure in this channel (Figure 22B-C).
The relative mRNA expression levels showed an increase in expression of mesenchymal markers, SNAI1, ZEB1 and MUC1 for both fluid flow conditions compared to the control without a fluid flow. (Figure 23). Vimentin expression was only increased for the tubule seeding method. These results show that the fluid flow induces the expression of EMT markers in CCA organoids.

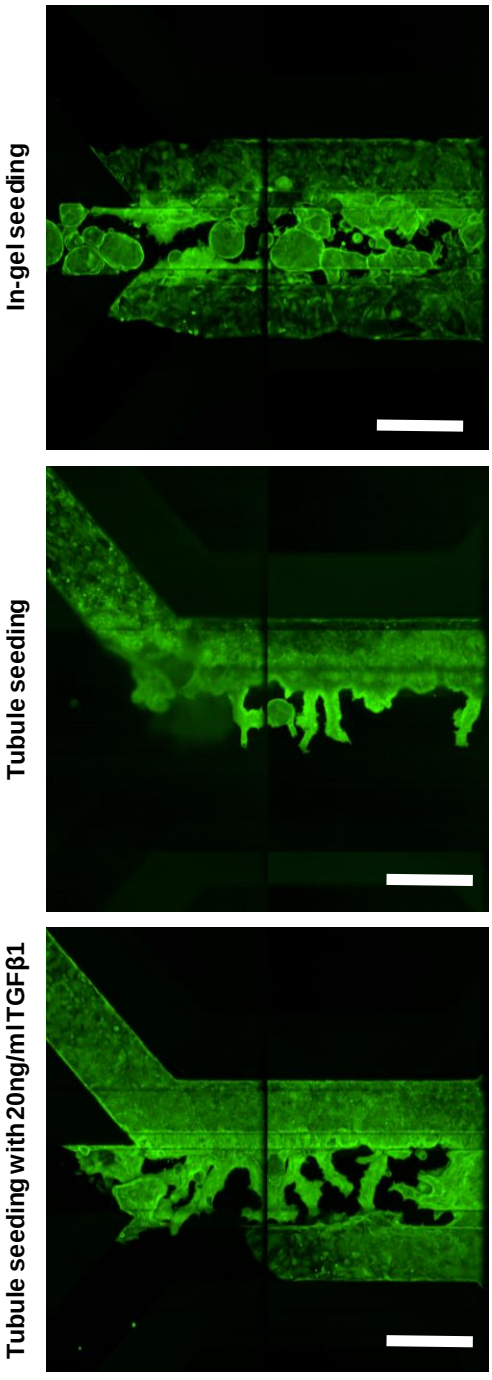

Figure 21: Maximum intensity projection of CCA1 organoids cultured in 3-lane Organoplate. In-gel seeding culture method: Cells grew into organoids in the middle BME channel. Subsequently, cells migrated to the medium channels. Tubule seeding culture method: Cells formed a tube in the top medium channel and protrusions in the middle channel. Tubule seeding culture method with 20ng/ml TGF-β1: Cells migrate from the top channel through the middle channel to the bottom channel (scale bar is 500µm).

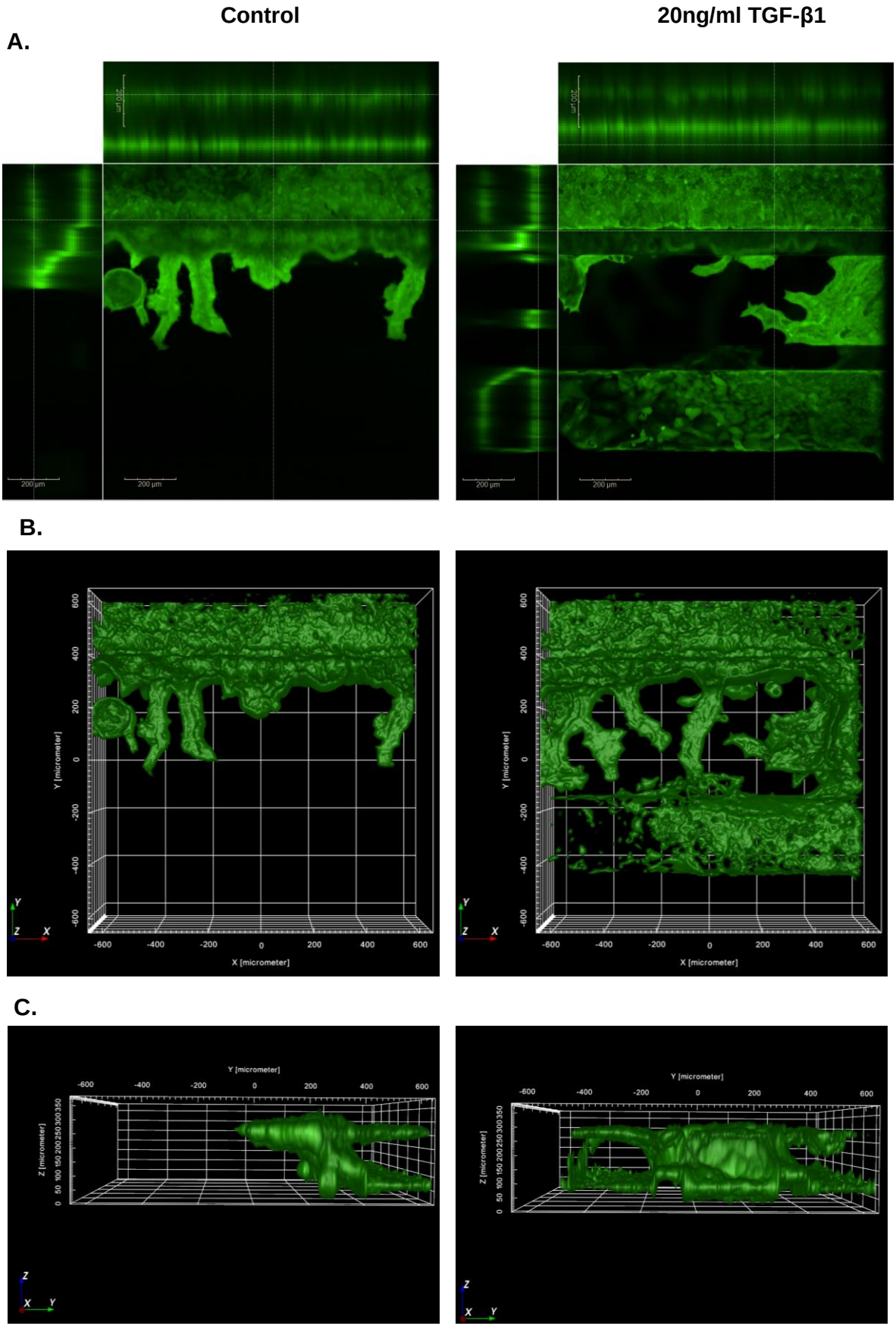

Figure 22: Tubule seeding culture method analysis. A: XYZ-plane of CCA1 organoids treated with and without TGF-β1 (scale bar is 200µm). **B&C:** 3D analysis of CCA1 organoids treated with and without TGF-β1. (B) Top view (XY) and (C) side view (YZ) images show the growth of CCA1 organoids after 8 days with a fluid flow rate of 121.2µl/h.

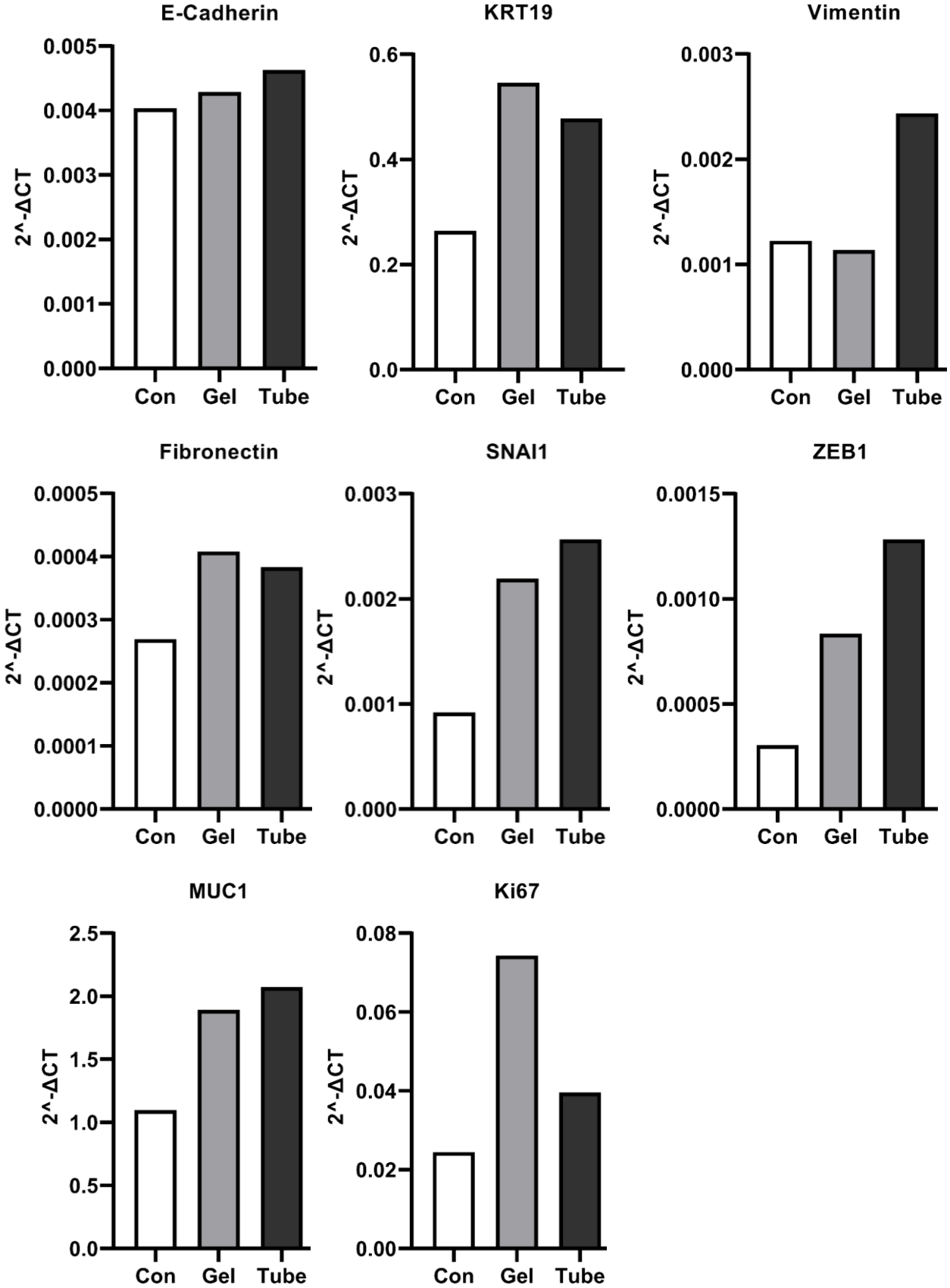

Figure 23: Quantitative real time PCR analysis of CCA organoids-on-a-chip. CCA organoids were cultured without a flow as a control (Con), with in-gel seeding method and a fluid flow (Gel) and with tubule seeding method and a fluid flow (Tube). The graphs show relative mRNA expression levels of epithelial markers (E-cadherin, KRT19), mesenchymal markers (Vimentin, Fibronectin, SNAI1, ZEB1, MUC1) and proliferation marker (Ki67). These graphs were normalized to GAPDH and HPRT.

4 DISCUSSION

Recently, Broutier et al. (10) have successfully established an organoid culture method for cells derived from CCA patients that provided new possibilities to develop novel *in vitro* CCA models including its *in vivo* physiology. Based on this method, we developed a novel organoid-based EMT model in CCA. Previous studies have demonstrated that growth factors, such as TGF-β1, TNF-α and IL-6, could stimulate EMT in multiple cancers including CCA [12, 13, 20]. The addition of various growth factors showed no significant morphological differences in CCA organoids. However, previous studies regarding EMT in CCA reported that cells change from cobblestone-like structures to spindle-like structures after growth factor treatment [9]. These studies were mainly limited to 2D culture methods that lack cell-cell interactions and are derived from single cell types. According to Sato et al. [12], only specific cell types undergo EMT whereas CCA organoids consist of various patient-specific epithelial cells. We suggest that only a small subset of CCA cells changes in phenotype, which could clarify the same round single layered epithelial morphology for all growth factor conditions, and a slight increase in mesenchymal gene expression. However, E-cadherin expression was also increased after growth factor treatment. Culturing CCA organoids in EM and BME could lead to induction of epithelial phenotype that is not easily overcome by addition of growth factors. Furthermore, CCA organoids were derived from patient-specific materials, and behaved differently under other culture conditions. CCA27 organoids only expressed E-cadherin, which could potentially be explained by a resistance to growth factors. Thus, CCA27 organoids were excluded from the experiments.

To further stimulate EMT, different culture media were used which showed that CCA organoids in EM changed from mono-layered epithelial 3D structures with a hollow lumen to small denser structures in TDM or branching structures in BM. Branching organoids in BM mimic the *in vivo* physiology more closely and showed the most substantial increase in expression of vimentin, fibronectin and SNAI1 after TGF-β1 treatment. It has been suggested that cells adopt EMT-like or mesenchymal-like phenotypes rather than complete EMT [12]. Additionally, Cadamuro et al. [33] have demonstrated that CCA cells express mesenchymal markers, but do not transdifferentiate into CAFs which is in accordance with our findings of increased expression of mesenchymal markers in CCA organoids that was different from expression in CAFs.

Although organoid cultures provide new *in vitro* model possibilities, they do not include all critical aspects of the tumor microenvironment. Organoids do not only lack cellular components such as immune cells and blood vessels, but also lack a native tumor ECM. The currently used hydrogels do not mimic biomechanical and biochemical complexity of the native ECM [34]. The development of the decellularization protocol in our lab allowed us to mimic the tumor microenvironment more closely by using patient-derived ECM scaffolds [26]. Tumor scaffolds were stiffer and thicker than donor scaffolds which is in line with the characteristics of ECM found in CCA and healthy tissues [35]. The ECM of CCA gradually changes from a thin layer into a rigid and thick structure with an increased stiffness stimulating tumor invasiveness and progression [35]. The reorganization and stiffening of the ECM has been associated with a poor prognosis in multiple cancers [36-38]. Another hallmark of CCA is the desmoplastic microenvironment containing fibrous connective tissue [39] which could clarify our findings that cells did only grow on specific locations in tumor scaffolds. The addition of TGF-β1 to the scaffold culture stimulated cells to adopt more mesenchymal-like morphology with gaps in the scaffolds. Manzaneres, et al. [40] have demonstrated that TGF-β1 stimulates desmoplastic phenotype in 3D CCA rat culture models. TGF-β1 promotes rearrangement of the cellular structure, which is in accordance with our results of various cell nucleus sizes and disorganized F-actin filaments after TGF-β1 treatment for both donor and tumor ECM scaffolds.

Besides F-actin filaments, intermediate filaments related proteins, such as vimentin, play a crucial role in the cytoskeleton of mesenchymal cells. Vimentin is typically located around the cell nucleus, which is in contrast to our findings of vimentin located in cell nucleus in both donor and tumor ECM scaffolds. The detected vimentin signal could be a background signal or a signal obtained from vimentin staining that was not completely washed away from the ECM scaffold. To draw firm conclusions, the protocol for vimentin staining in ECM scaffolds should be optimized. Furthermore, it is recommended to stain the cell nucleus, F-actin and vimentin in one sample to determine the location of the components and change in morphology more easily. Culturing CAFs on an ECM scaffold could not only validate the vimentin staining protocol, but also provide a positive control for RNA expression levels. Vimentin expression along with other EMT markers in ECM scaffolds were higher compared to expression in CCA organoids cultured in BME. However, we did not observe significant differences in expression of EMT markers between donor and tumor ECM scaffolds. Depending on specific combinations of organoids and scaffolds, an increase of mesenchymal markers was observed. Similar results were found in colorectal cancer research which have demonstrated that the use of patient-derived scaffolds provides patient-specific outcome [34].

The change in ECM composition contributes to EMT activation and tumor invasion that is also correlated with modulation of fluid flow [27]. Microfluidics enabled us to explore the effect of fluid flow *in vitro* by developing a CCA-on-a-chip model. We observed that the presence of a fluid flow stimulated migration of CCA organoids into the culture medium. Previous studies have demonstrated that interstitial fluid flow is not only involved in passive transport and dissemination of tumor cells, but also involved in promoting migration in various cancers [41]. Interestingly, CCA cells were able to adopt a tube structure due to a fluid flow. Subsequently, cells migrated and formed protrusions which was accelerated by TGF-β1 treatment. Prior research suggested that fluid flow increases TGF-β1 activation by improving its transport, while cancer cells were indirectly stimulated by TGF-β1 [42]. Comparing to the static condition, we observed altered expression of EMT markers in CCA organoids under flow conditions which was also found in ovarian and breast cancer [30, 43]. However, our flow-induced experiments were limited to one CCA organoid line which has to be extended to validate the significance of the fluid flow on the induction of EMT.

4.1 Future recommendations

Our organoid-based EMT in CCA model provided a foundation to study EMT in CCA organoids including the effect of growth factors, native ECM and fluid flow. However, further research on EMT in CCA is still required to strengthen the existing data. It is recommended to expand the number of patient-specific cell and ECM sources in this study. The use of more CCA patient material could aid in the development of patient-specific models that opens the door to personalized medicine. Regarding the flow-induced EMT model, the next step is to optimize the culture medium and flow rate for EMT activation. The existing data could be extended by visualizing the cell morphology with staining such as DAPI (cell nucleus), phalloidin (F-actin) or ZO-1 (tight-junctions). The implementation of CCA organoids with other cellular components, such as CAFs and TAMs, in a direct co-culture model enables to study the *in vivo* complexity of CCA. To advance the development of an EMT model, combining cellular components as well as mechanical factors of the tumor microenvironment in an *in vitro* experimental model allow for more incorporation of the native tumor microenvironment that could lead to better representation and possibly a deeper insight into EMT behavior.

5 CONCLUSION

In this study, we provided a foundation for a novel *in vitro* organoid-based epithelial-mesenchymal transition model in cholangiocarcinoma including the initial tumor characteristics and tumor microenvironment. EMT activation in CCA organoids was examined by using three different aspects of the tumor microenvironment.

1. *What are the effects of different EMT promoting growth factors and culture media on the activation of EMT in CCA organoids cultured in BME?*

Different concentrations and combinations of TGF-β1, TNF-α and IL-6 were added to CCA organoids which showed no significant morphological differences between the growth factor conditions. However, we observed a slight increase in the relative mRNA expression of mesenchymal markers such as vimentin, fibronectin and SNAI1 after TGF-β1 and/or TNF-α treatment. Additionally, the medium composition of BM enhanced expression of mesenchymal markers after TGF-β1 treatment, and mimicked the initial tumor better than in EM and TDM. The combined optimal treatment of TGF-β1/TNF-α and BM resulted in downregulation of E-cadherin gene expression (epithelial marker) and upregulation of mesenchymal markers. Our findings suggest that TGF-β1/TNF-α treatment and BM could aid in EMT activation.

2. *What is the effect of the tumor extracellular matrix on EMT activation in CCA organoids?*

The present study investigated the effect of the ECM on EMT activation by using patient-derived donor and tumor ECM scaffolds. Our results indicated morphological changes of cells after TGF-β1 treatment in BM. Cells with polygonal cell shape and regular cell nucleus dimensions changed to irregular cell shape and cell nucleus after TGF-β1 treatment. Based on the relative mRNA expression in donor and tumor ECM, only a significant difference was observed for fibronectin expression in donor ECM. However, specific combinations of cell and ECM sources showed downregulation of epithelial gene expressions and upregulation of mesenchymal gene expressions after TGF-β1 treatment, which indicates the activation of EMT. Therefore, we propose that patient-specific ECM could aid in stimulation of EMT in CCA organoids.

3. *What is the effect of the interstitial fluid flow on EMT activation in CCA organoids?*

We developed a CCA organoid-on-a-chip model to examine whether the interstitial fluid flow could stimulate EMT induction. CCA organoids were cultured with three different seeding methods in a microfluidic platform. Similar to the static condition, cells did grow into organoids in the presence of a flow. However, cells also migrated to the other medium

channels. Interestingly, cells were also able to form a tube structure with protrusions outwards to the BME channel in which the migration process was accelerated by TGF-β1 treatment. Furthermore, the gene expression levels of EMT markers were induced in the presence of a flow. Our results have demonstrated that the fluid flow could potentially stimulate EMT in CCA organoids.

Although our *in vitro* EMT model does not fully capture the complexity of CCA, it recapitulates the *in vivo* tumor physiology more closely than 2D culture methods. The use of patient-specific organoids, patient-specific ECM and microfluidics provided a basis to develop a more representative *in vitro* EMT model for CCA organoids, including its characteristics and tumor microenvironment. Our model could not only aid in understanding chemoresistance, but could also enable us to better understand and model the underlying mechanism of CCA and its progression.

6
ACKNOWLEDGEMENT

This project was made possible thanks to the support of various individuals with expertise in this research field. First, I would like to thank my daily supervisor, Gilles van Tienderen, for guiding and supporting me during this project. He was always happy to help and to answer all my questions. I would also like to thank my Erasmus MC supervisor, Monique Verstegen, and Luc van der Laan for welcoming me warmly and giving me the opportunity to join their research group. The ambiance in the lab was motivating due to wonderful and helpful lab members. Thanks to all lab members, especially Kübra Köten for preparing my culture media and Kathryn Monfils for helping me using the confocal microscopy. I would also like to thank my TU Delft supervisor, Lidy Fratila-Apachitei, for providing guidance and feedback from the TU Delft. Furthermore, I would like to thank all members of the graduation committee.

7 ABBREVIATIONS

BME	Basement membrane matrix
BM	Branching medium
CAF	Cancer associated fibroblast
CCA	Cholangiocarcinoma
DAPI	4,6-diamidino-2-phenylindole
ECM	Extracellular matrix
EM	Expansion medium
EMT	Epithelial-mesenchymal transition
H&E	Haematoxylin and eosin
IL-6	Interleukin 6
OCT	Optimal cutting temperature
Rpm	Revolutions per minute
PBS	Phosphate-buffered saline
P/S	Penicillin-streptomycin
SD	Standard deviation
TAM	Tumor associated macrophage
TDM	Tumor differentiation medium
TGF-β1	Transforming growth factor beta 1
TNF-α	Tumor necrosis factor alpha

8

REFERENCES

[1] J. M. Banales, J. J. G. Marin, A. Lamarca, P. M. Rodrigues, S. A. Khan, L. R. Roberts*, et al.*, "Cholangiocarcinoma 2020: the next horizon in mechanisms and management," *Nature Reviews Gastroenterology & Hepatology,* vol. 17, pp. 557-588, 2020/09/01 2020.

[2] A. Dongre and R. A. Weinberg, "New insights into the mechanisms of epithelial–mesenchymal transition and implications for cancer," *Nature Reviews Molecular Cell Biology,* vol. 20, pp. 69-84, 2019/02/01 2019.

[3] P. Dasgupta, C. Henshaw, D. R. Youlden, P. J. Clark, J. F. Aitken, and P. D. Baade, "Global Trends in Incidence Rates of Primary Adult Liver Cancers: A Systematic Review and Meta-Analysis," *Frontiers in oncology,* vol. 10, pp. 171-171, 2020.

[4] F. Bray, J. Ferlay, I. Soerjomataram, R. L. Siegel, L. A. Torre, and A. Jemal, "Global cancer statistics 2018: GLOBOCAN estimates of incidence and mortality worldwide for 36 cancers in 185 countries," *CA: A Cancer Journal for Clinicians,* vol. 68, pp. 394-424, 2018/11/01 2018.

[5] J. M. Banales, V. Cardinale, G. Carpino, M. Marzioni, J. B. Andersen, P. Invernizzi*, et al.*, "Cholangiocarcinoma: current knowledge and future perspectives consensus statement from the European Network for the Study of Cholangiocarcinoma (ENS-CCA)," *Nature Reviews Gastroenterology & Hepatology,* vol. 13, pp. 261-280, 2016/05/01 2016.

[6] B. Blechacz, M. Komuta, T. Roskams, and G. J. Gores, "Clinical diagnosis and staging of cholangiocarcinoma," *Nat Rev Gastroenterol Hepatol,* vol. 8, pp. 512-22, Aug 2 2011.

[7] A. Forner, G. Vidili, M. Rengo, L. Bujanda, M. Ponz-Sarvisé, and A. Lamarca, "Clinical presentation, diagnosis and staging of cholangiocarcinoma," *Liver Int,* vol. 39 Suppl 1, pp. 98-107, May 2019.

[8] J. L. A. van Vugt, M. P. Gaspersz, R. J. S. Coelen, J. Vugts, T. A. Labeur, J. de Jonge*, et al.*, "The prognostic value of portal vein and hepatic artery involvement in patients with perihilar cholangiocarcinoma," *HPB (Oxford),* vol. 20, pp. 83-92, Jan 2018.

[9] J. Vaquero, N. Guedj, A. Clapéron, T. H. Nguyen Ho-Bouldoires, V. Paradis, and L. Fouassier, "Epithelial-mesenchymal transition in cholangiocarcinoma: From clinical evidence to regulatory networks," *J Hepatol,* vol. 66, pp. 424-441, Feb 2017.

[10] L. Broutier, G. Mastrogiovanni, M. M. Verstegen, H. E. Francies, L. M. Gavarró, C. R. Bradshaw*, et al.*, "Human primary liver cancer-derived organoid cultures for disease modeling and drug screening," *Nat Med,* vol. 23, pp. 1424-1435, Dec 2017.

[11] M. guarino, B. rubino, and g. ballabio, "The role of epithelial-mesenchymal transition in cancer pathology," *Pathology,* vol. 39, pp. 305-318, 2007/06/01/ 2007.

[12] Y. Sato, K. Harada, K. Itatsu, H. Ikeda, Y. Kakuda, S. Shimomura*, et al.*, "Epithelial-Mesenchymal Transition Induced by Transforming Growth Factor-β1/Snail Activation Aggravates Invasive Growth of Cholangiocarcinoma," *The American Journal of Pathology,* vol. 177, pp. 141-152, 2010/07/01/ 2010.

[13] Z.-Y. Shuang, W.-C. Wu, J. Xu, G. Lin, Y.-C. Liu, X.-M. Lao*, et al.*, "Transforming growth factor-β1-induced epithelial–mesenchymal transition generates ALDH-positive cells with stem cell properties in cholangiocarcinoma," *Cancer Letters,* vol. 354, pp. 320-328, 2014/11/28/ 2014.

[14] K. Araki, T. Shimura, H. Suzuki, S. Tsutsumi, W. Wada, T. Yajima*, et al.*, "E/N-cadherin switch mediates cancer progression via TGF-β-induced epithelial-to-mesenchymal transition in extrahepatic cholangiocarcinoma," *British Journal of Cancer,* vol. 105, pp. 1885-1893, 2011/12/01 2011.

[15] K. Duangkumpha, A. Techasen, W. Loilome, N. Namwat, R. Thanan, N. Khuntikeo*, et al.*, "BMP-7 blocks the effects of TGF-β-induced EMT in cholangiocarcinoma," *Tumor Biology,* vol. 35, pp. 9667-9676, 2014/10/01 2014.

[16] G. Tzanakakis, R.-M. Kavasi, K. Voudouri, A. Berdiaki, I. Spyridaki, A. Tsatsakis*, et al.*, "Role of the extracellular matrix in cancer-associated epithelial to mesenchymal transition phenomenon," *Developmental Dynamics,* vol. 247, pp. 368-381, 2018/03/01 2018.

[17] G. S. van Tienderen, B. Groot Koerkamp, J. N. M. Ijzermans, L. J. W. van der Laan, and M. M. A. Verstegen, "Recreating Tumour Complexity in a Dish: Organoid Models to Study Liver Cancer Cells and their Extracellular Environment," *Cancers,* vol. 11, p. 1706, 2019.

[18] V. Papalazarou, M. Salmeron-Sanchez, and L. M. Machesky, "Tissue engineering the cancer microenvironment—challenges and opportunities," *Biophysical Reviews,* vol. 10, pp. 1695-1711, 2018/12/01 2018.

[19] A. Techasen, W. Loilome, N. Namwat, N. Khuntikeo, A. Puapairoj, P. Jearanaikoon*, et al.*, "Loss of E-cadherin promotes migration and invasion of cholangiocarcinoma cells and serves as a potential marker of metastasis," *Tumor Biology,* vol. 35, pp. 8645-8652, 2014/09/01 2014.

[20] Q.-X. Zhou, X.-M. Jiang, Z.-D. Wang, C.-L. Li, and Y.-F. Cui, "Enhanced expression of suppresser of cytokine signaling 3 inhibits the IL-6-induced epithelial-to-mesenchymal transition and cholangiocarcinoma cell metastasis," *Medical Oncology,* vol. 32, p. 105, 2015/03/06 2015.

[21] J. He, X. Zhang, X. Xia, M. Han, F. Li, C. Li*, et al.*, "Organoid technology for tissue engineering," *Journal of Molecular Cell Biology,* vol. 12, pp. 569-579, 2020.

[22] S. Vicent, R. Lieshout, A. Saborowski, M. M. A. Verstegen, C. Raggi, S. Recalcati*, et al.*, "Experimental models to unravel the molecular pathogenesis, cell of origin and stem cell properties of cholangiocarcinoma," *Liver Int,* vol. 39 Suppl 1, pp. 79-97, May 2019.

[23] S. Hahn, M. O. Nam, J. H. Noh, D. H. Lee, H. W. Han, D. H. Kim*, et al.*, "Organoid-based epithelial to mesenchymal transition (OEMT) model: from an intestinal fibrosis perspective," *Sci Rep,* vol. 7, p. 2435, May 26 2017.

[24] J. S. Lee, J. Shin, H.-M. Park, Y.-G. Kim, B.-G. Kim, J.-W. Oh*, et al.*, "Liver Extracellular Matrix Providing Dual Functions of Two-Dimensional Substrate Coating and Three-Dimensional Injectable Hydrogel Platform for Liver Tissue Engineering," *Biomacromolecules,* vol. 15, pp. 206-218, 2014/01/13 2014.

[25] F. d. Weijer, "Modeling Primary Liver Cancer using Tumor-Derived Extracellular Matrix," TU Delft & Erasmus MC, 2019.

[26] J. Willemse, R. Lieshout, L. J. W. van der Laan, and M. M. A. Verstegen, "From organoids to organs: Bioengineering liver grafts from hepatic stem cells and matrix," *Best Pract Res Clin Gastroenterol,* vol. 31, pp. 151-159, Apr 2017.
[27] J. M. Munson and A. C. Shieh, "Interstitial fluid flow in cancer: implications for disease progression and treatment," *Cancer management and research,* vol. 6, pp. 317-328, 2014.
[28] S. Evje and J. O. Waldeland, "How Tumor Cells Can Make Use of Interstitial Fluid Flow in a Strategy for Metastasis," *Cell Mol Bioeng,* vol. 12, pp. 227-254, Jun 2019.
[29] A. S. Piotrowski-Daspit, J. Tien, and C. M. Nelson, "Interstitial fluid pressure regulates collective invasion in engineered human breast tumors via Snail, vimentin, and E-cadherin," *Integrative biology : quantitative biosciences from nano to macro,* vol. 8, pp. 319-331, 2016.
[30] I. Rizvi, U. A. Gurkan, S. Tasoglu, N. Alagic, J. P. Celli, L. B. Mensah*, et al.*, "Flow induces epithelial-mesenchymal transition, cellular heterogeneity and biomarker modulation in 3D ovarian cancer nodules," *Proceedings of the National Academy of Sciences,* vol. 110, p. E1974, 2013.
[31] C. Beaurivage, A. Kanapeckaite, C. Loomans, K. S. Erdmann, J. Stallen, and R. A. J. Janssen, "Development of a human primary gut-on-a-chip to model inflammatory processes," *Scientific Reports,* vol. 10, p. 21475, 2020/12/08 2020.
[32] Mimetas. (February 1). *Technology*. Available: https://mimetas.com/page/technology
[33] M. Cadamuro, G. Nardo, S. Indraccolo, L. Dall'olmo, L. Sambado, L. Moserle*, et al.*, "Platelet-derived growth factor-D and Rho GTPases regulate recruitment of cancer-associated fibroblasts in cholangiocarcinoma," *Hepatology,* vol. 58, pp. 1042-53, Sep 2013.
[34] G. Parkinson, S. Salerno, P. Ranji, J. Håkansson, Y. Bogestål, Y. Wettergren*, et al.*, "Patient-derived scaffolds as a model of colorectal cancer," *Cancer Medicine,* vol. 10, 2020.
[35] M. Cadamuro, T. Stecca, S. Brivio, V. Mariotti, R. Fiorotto, C. Spirli*, et al.*, "The deleterious interplay between tumor epithelia and stroma in cholangiocarcinoma," *Biochimica et Biophysica Acta (BBA) - Molecular Basis of Disease,* vol. 1864, pp. 1435-1443, 2018/04/01/ 2018.
[36] H. Yu, J. K. Mouw, and V. M. Weaver, "Forcing form and function: biomechanical regulation of tumor evolution," *Trends Cell Biol,* vol. 21, pp. 47-56, Jan 2011.
[37] K. R. Levental, H. Yu, L. Kass, J. N. Lakins, M. Egeblad, J. T. Erler*, et al.*, "Matrix crosslinking forces tumor progression by enhancing integrin signaling," *Cell,* vol. 139, pp. 891-906, Nov 25 2009.
[38] S. Kumar and V. M. Weaver, "Mechanics, malignancy, and metastasis: the force journey of a tumor cell," *Cancer Metastasis Rev,* vol. 28, pp. 113-27, Jun 2009.
[39] J. I. Lee and J. S. Campbell, "Role of desmoplasia in cholangiocarcinoma and hepatocellular carcinoma," *Journal of Hepatology,* vol. 61, pp. 432-434, 2014/08/01/ 2014.
[40] M. Á. Manzanares, A. Usui, D. J. Campbell, C. I. Dumur, G. T. Maldonado, M. Fausther*, et al.*, "Transforming Growth Factors α and β Are Essential for Modeling Cholangiocarcinoma Desmoplasia and Progression in a Three-Dimensional Organotypic Culture Model," *The American Journal of Pathology,* vol. 187, pp. 1068-1092, 2017/05/01/ 2017.
[41] W. J. Polacheck, A. E. German, A. Mammoto, D. E. Ingber, and R. D. Kamm, "Mechanotransduction of fluid stresses governs 3D cell migration," *Proc Natl Acad Sci U S A,* vol. 111, pp. 2447-52, Feb 18 2014.
[42] A. C. Shieh, H. A. Rozansky, B. Hinz, and M. A. Swartz, "Tumor cell invasion is promoted by interstitial flow-induced matrix priming by stromal fibroblasts," *Cancer Res,* vol. 71, pp. 790-800, Feb 1 2011.
[43] A. M. Tchafa, M. Ta, M. J. Reginato, and A. C. Shieh, "EMT Transition Alters Interstitial Fluid Flow-Induced Signaling in ERBB2-Positive Breast Cancer Cells," *Mol Cancer Res,* vol. 13, pp. 755-64, Apr 2015.

9

SUPPLEMENTARY

9.1 Genomic profile of CCA organoids

Table 5: Genomic profile of CCA organoids.

Organoid	Mutations		Chromosomal imbalance	
			Loss	Gain
CCA1 Perihilar	ARID1A IGF1R KRAS	p.Arg1989Ter splicing p.Gly12Asp	CDKN2A (homozygous)	
CCA14 Intrahepatic	BAP1	p.Pro190Thr	MTOR ARID1A NRAS CTNNB1 BAP1 CDKN2A (homozygous)	MYC PTEN IGF1R ERBB2 RNF43
CCA27 Intrahepatic	KRAS TP53	p.Gly12Asp p.Ala347Thr	ARID1A VHL CTNNB1 BAP1 FHIT PIK3R1 ROS1 FGFR1 CDKN2A TP53 SMAD4	DDR2 MYC IGF1R

9.2 Culture medium composition

Various cell culture media were used for different experiments. The medium compositions with a total volume of 1ml are shown in Table 6 and Table 7. AdF12^{++++} contains AdF12 (base medium) with P/S (1%), Primocin (50 µg/ml), Ultraglutamine (1%) and Hepes (10mM). In some experiments, expansion medium was used without A8301 (Ti) due to the inhibition of TGF-β1. A8301(Ti) was substituted by AdF12^{++++}. The composition of the branching medium (BM) is confidential and therefore not included.

Table 6: Composition of expansion medium (EM).

Component	Volume (µl)	Final concentration
AdF12^{++++}	852.5	
N2	10	
B27	20	
Gastrin I	1	10nM
FGF10	1	100ng/ml
HGF	0.5	25ng/ml
EGF	1	50ng/ml
A8301(Ti)	1	5µM
Nicotinamide	10	10mM
Forskolin	1	10µM
Ac Cys	2	1mM
RSPo CM	100	

Table 7: Composition of tumor differentiation medium (TDM).

Component	Volume (µl)	Final concentration
AdF12^{++++}	963.5	
N2	10	
B27	20	
Gastrin I	1	10nM
FGF10	1	100ng/ml
HGF	0.5	25ng/ml
EGF	1	50ng/ml
Ac Cys	2	1mM
Dex	1	30µM

9.3 Primer design

Several primers were designed for quantitative RT-PCR analysis as shown in Table 8.

Table 8: Overview of primers

Primer name	Forward primer	Reverse primer
KRT19	GCACTACAGCCACTACTACACGA	CTCATGCGCAGAGCCTGTT
E-cadherin	CTGGACAGGGAGGATTTTGA	ACCTGAGGCTTTGGATTCCT
Fibronectin	TGCACATGCTTTGGAGGCCA	GCATGAAGCACTCAATTGGGCA
HPRT	ACCAGTCAACAGGGGACATAA	CTTCGTGGGGTCCTTTTCACC
GAPDH	CTTTTGCGTCGCCAGCCGAG	CCAGGCGCCCAATACGACCA
Ki67	CTACGGATTATACCTGGCCTTCC	AGGAAGCTGGATACGGATGTCA
MUC1	CTGTCAGTGCCGCCGAAAGA	CGTGCCCCTACAAGTTGGCA
SNAI1	TGCCCTCAAGATGCACATC	GGGACAGGAGAAGGGCTTC
Vimentin	CGGGAGAAATTGCAGGAGG	TGCTGTTCCTGAATCTGAGC

9.4 RNA expression in CCA organoids cultured on ECM scaffold

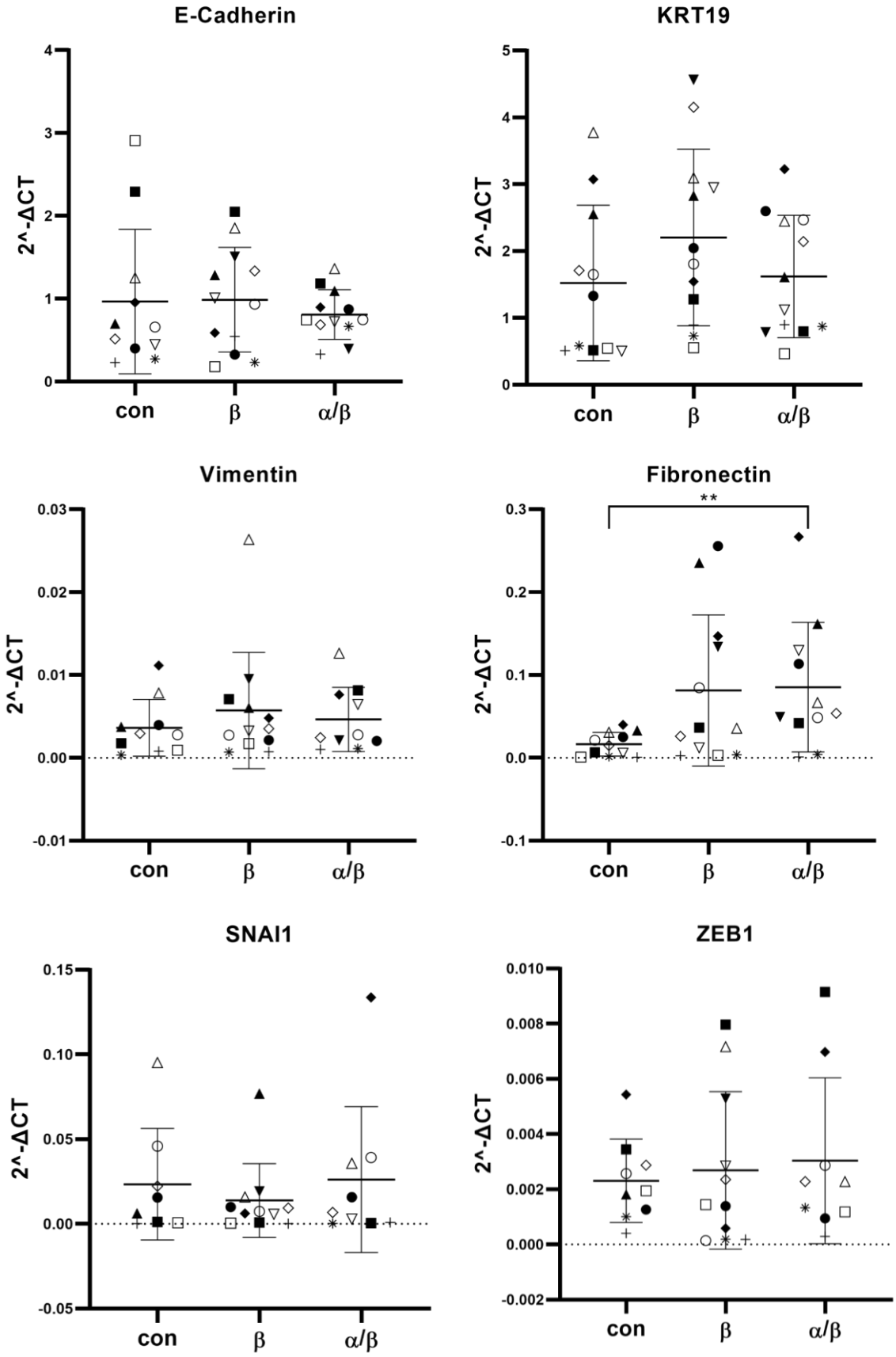

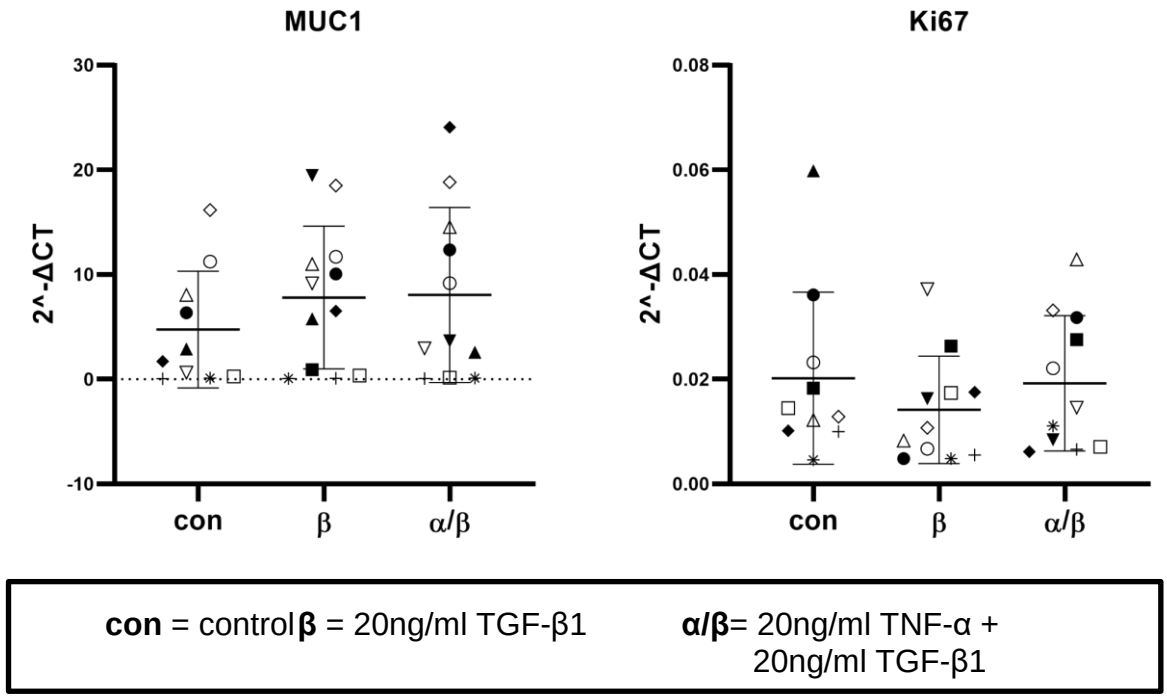

Figure 24: RNA expression in CCA organoids cultured on ECM scaffolds with BM. CCA organoids (n=2) were cultured on donor scaffolds (n=3) and tumor scaffolds (n=3). Both scaffolds were grouped together to show the overall effect of growth factors regardless of scaffold type. The graphs include twelve different conditions, each displayed with another symbol, and show relative mRNA expression levels of epithelial markers (E-cadherin, Cytokeratin), mesenchymal markers (Vimentin, Fibronectin, SNAI1, Zeb1, Muc1) and proliferation marker (Ki67). Data were normalized to GAPDH and HPRT and included mean ± SD with a Mann-Whitney U test (**p<0.01).

9.5 H&E staining of multiple scaffold sections

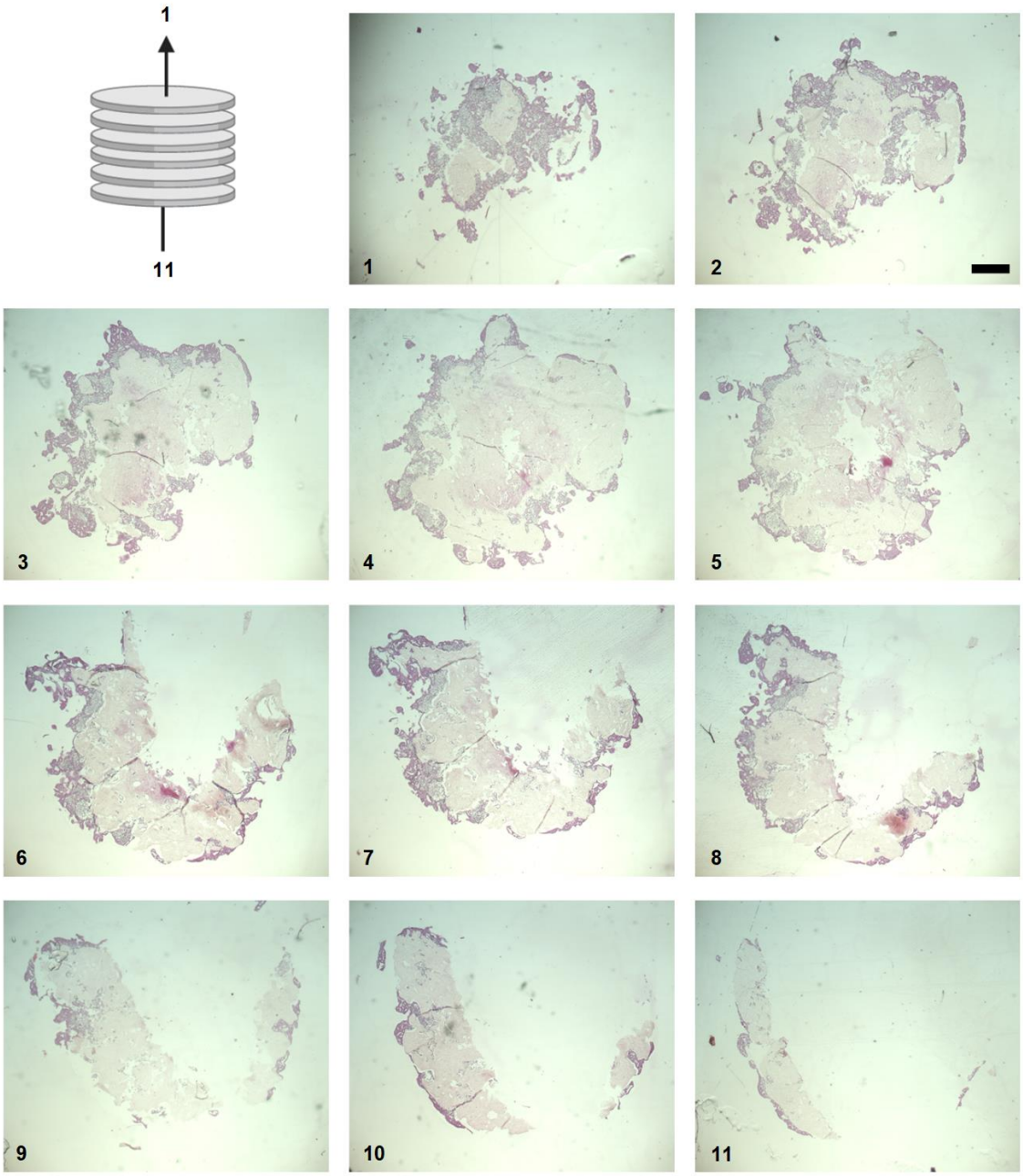

Figure 25: H&E staining of CCA14 organoids cultured in tumor (CCA1108) scaffold. Multiple paraffin sections were collected in a sequence. The schematic representation of the scaffold displays the direction of the sections through the scaffold. Image 1 is the top section and image 11 is the bottom section of the scaffold (scale bar is 100µm).

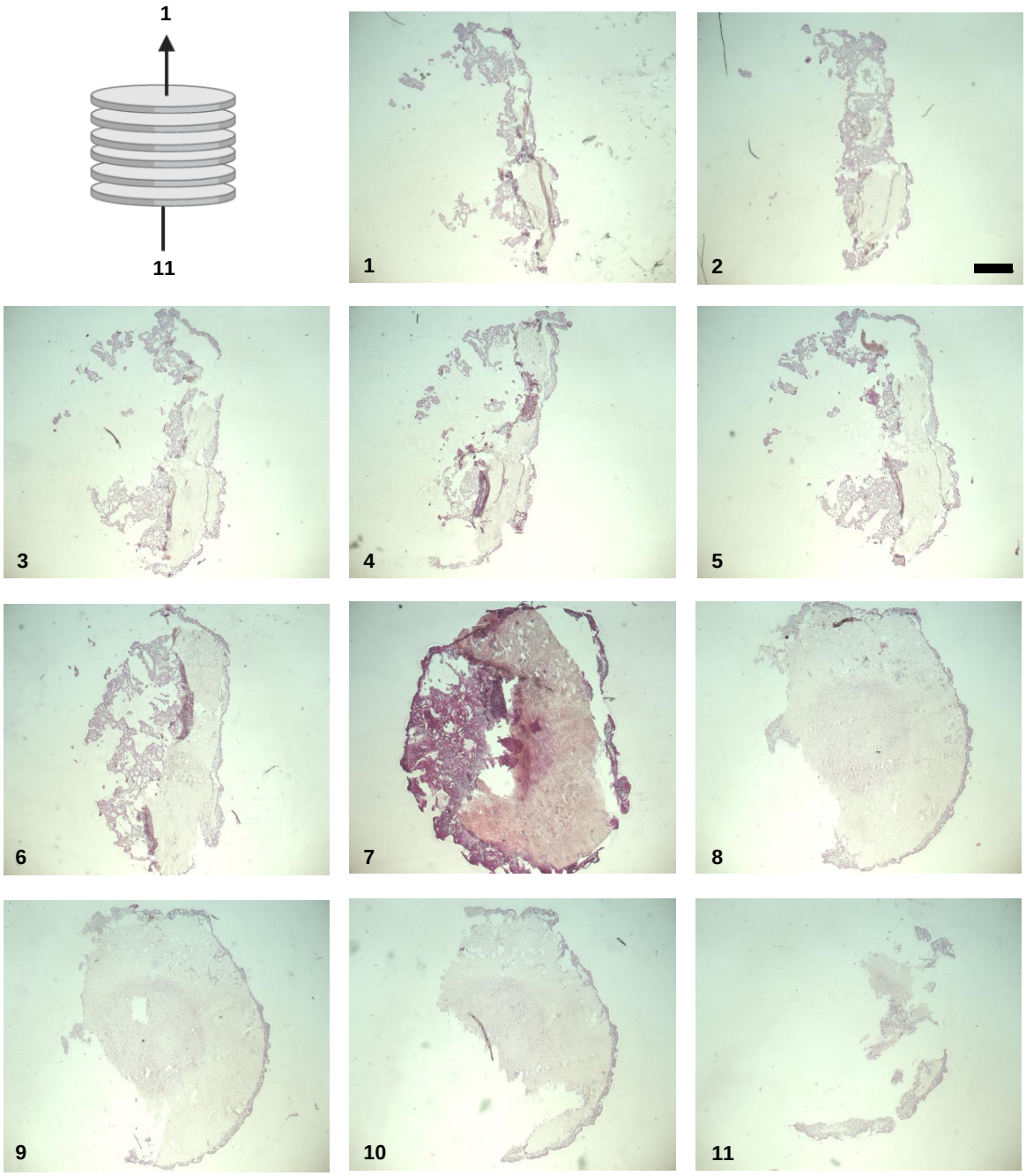

Figure 26: H&E staining of CCA14 organoids cultured in tumor (CCA1108) scaffold treated with 20ng/ml TGF-β1. Multiple paraffin sections were collected in a sequence. The schematic representation of the scaffold displays the direction of the sections through the scaffold. Image 1 is the top section and image 11 is the bottom section of the scaffold (scale bar is 100µm).

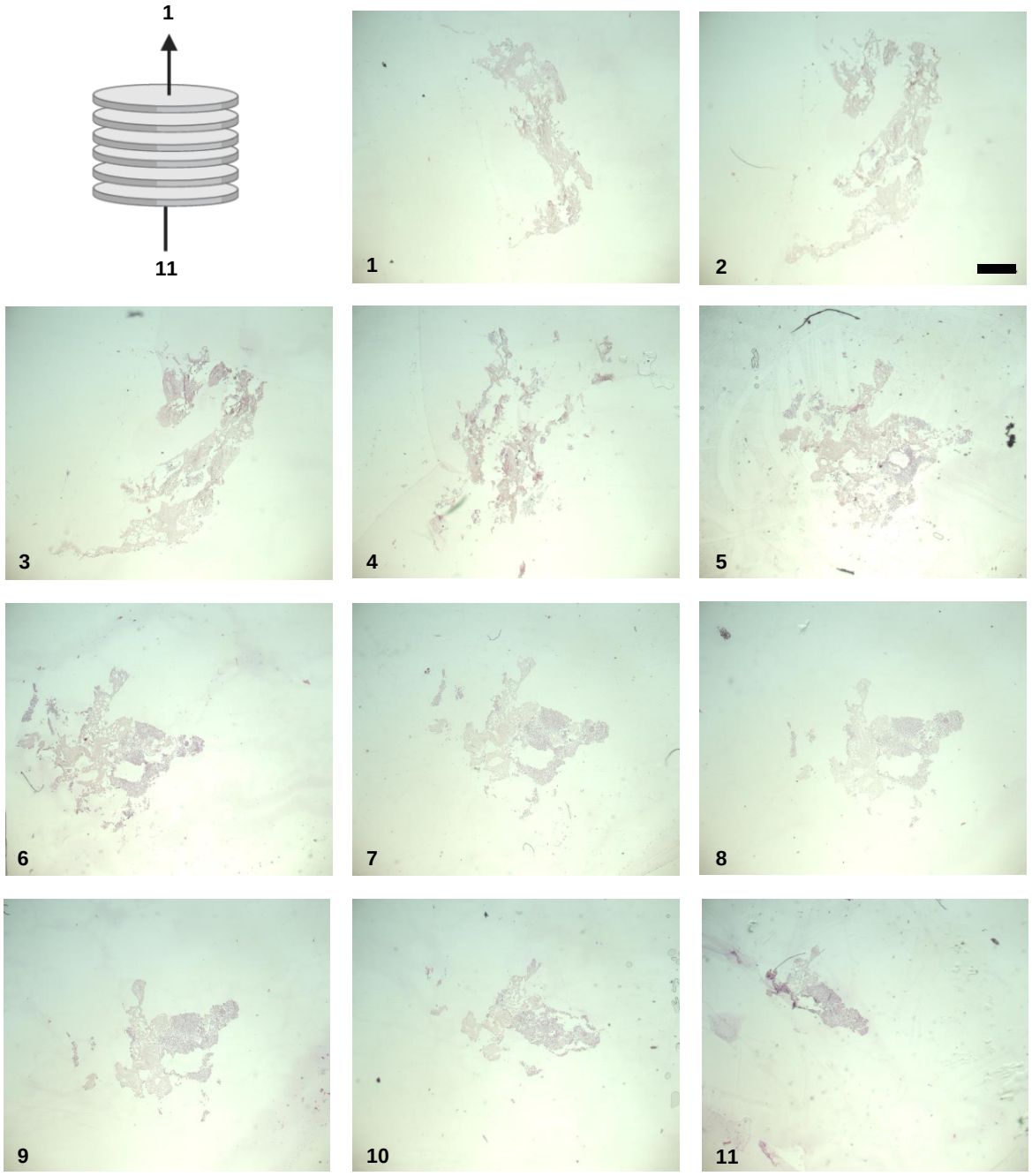

Figure 27: H&E staining of CCA14 organoids cultured in donor (H41) scaffold. Multiple paraffin sections were collected in a sequence. **T**he schematic representation of the scaffold displays the direction of the sections through the scaffold. Image 1 is the top section and image 11 is the bottom section of the scaffold (scale bar is 100µm).

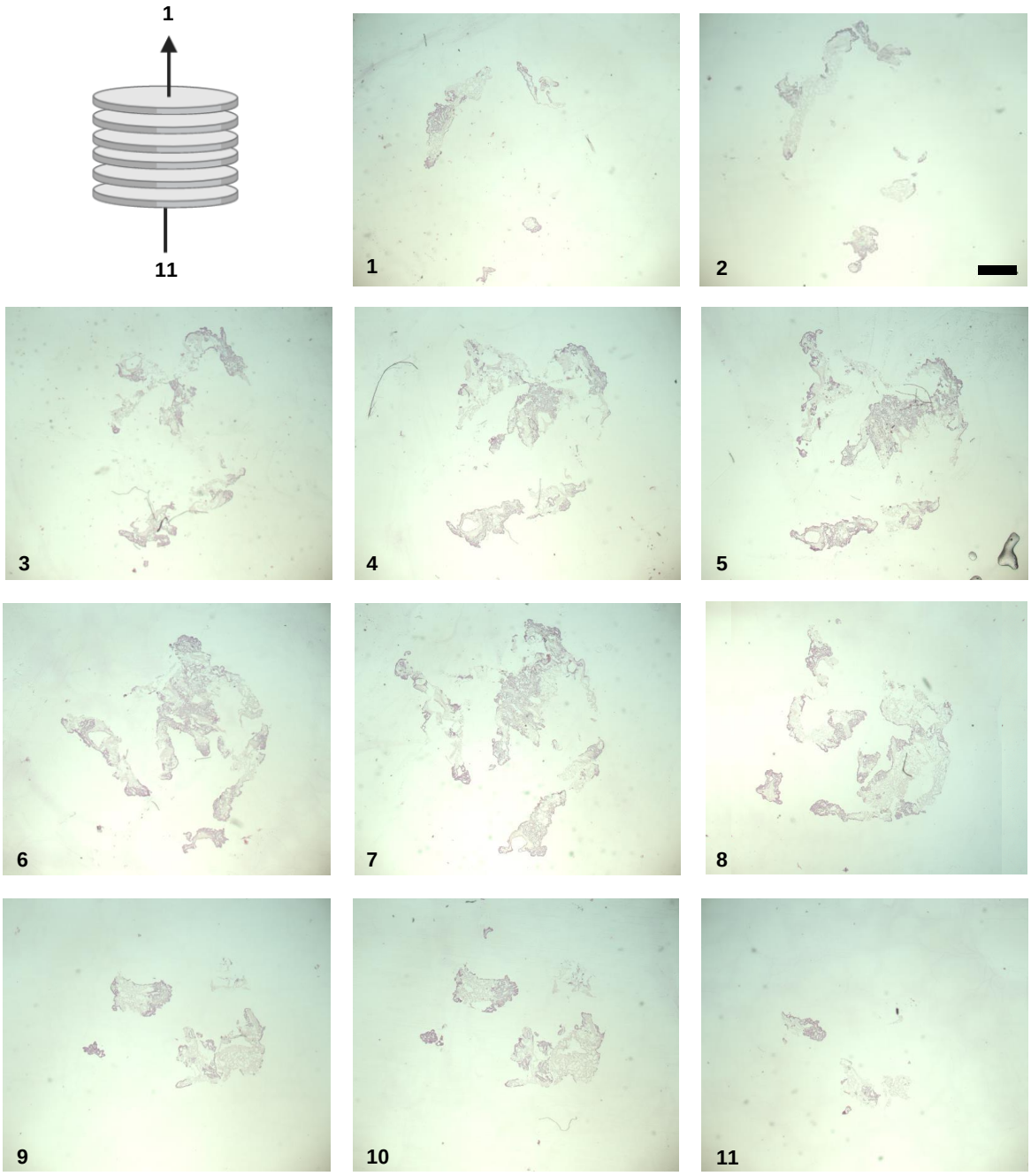

Figure 28: H&E staining of CCA14 organoids cultured in donor (H41) scaffold treated with 20ng/ml TGF-β1. Multiple paraffin sections were collected in a sequence. The schematic representation of the scaffold displays the direction of the sections through the scaffold. Image 1 is the top section and image 11 is the bottom section of the scaffold (scale bar is 100µm).

9.6 Maximum intensity projection of CCA organoids stained with DAPI, Phalloidin and Vimentin

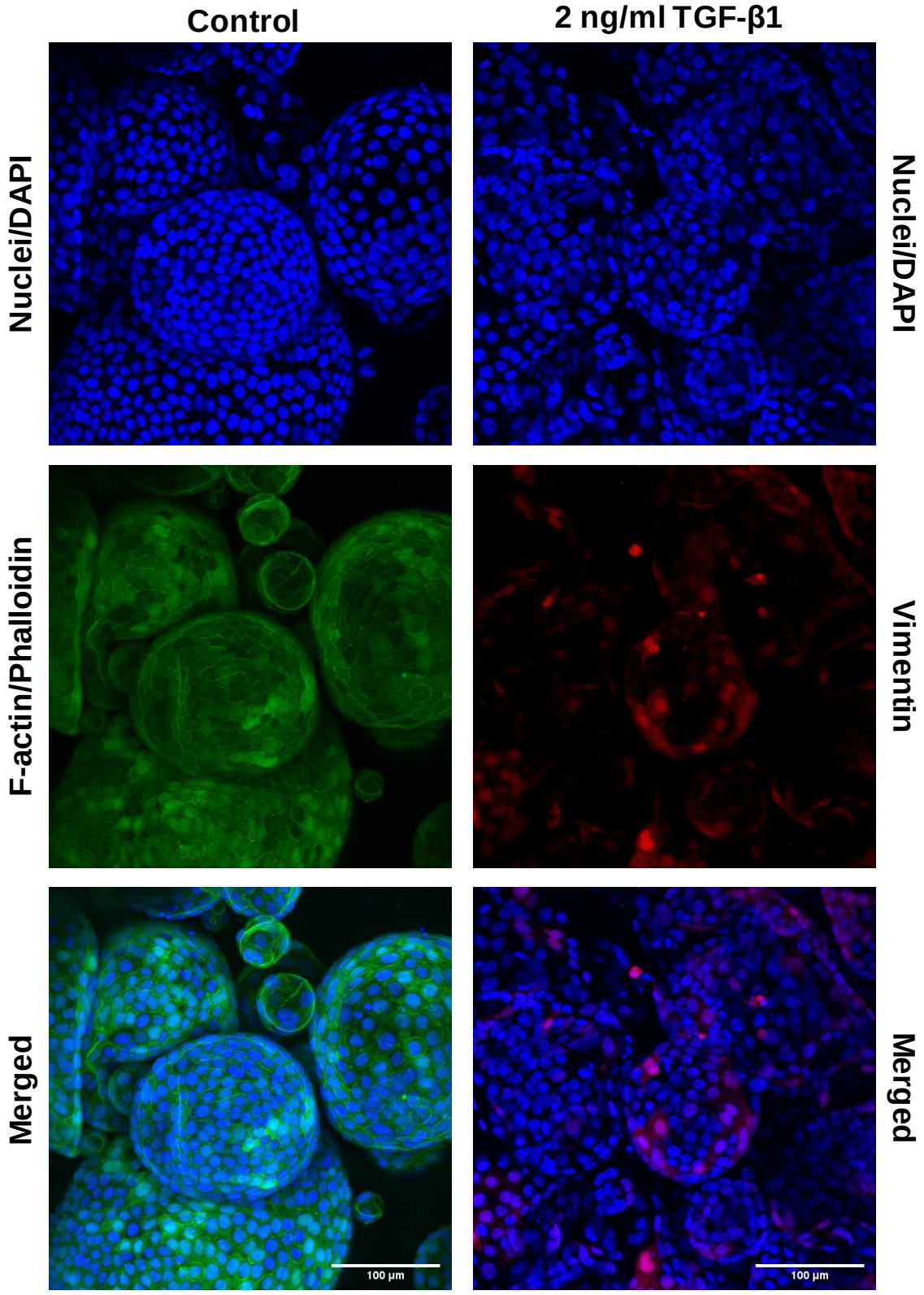

Figure 29: Maximum intensity projection of CCA14 organoids cultured in BME with EM- (control). Left: Organoids were cultured for 7 days. Images include cell nuclei (DAPI; blue) and F-actin (Phalloidin; green). Right: Organoids were treated with 2ng/ml TGF-β1 for 7 days. Images include cell nuclei (DAPI; blue) and vimentin (red) (scale bar is 100µm).

9.7 Vimentin staining of CCA organoids in tumor and donor scaffolds

A.

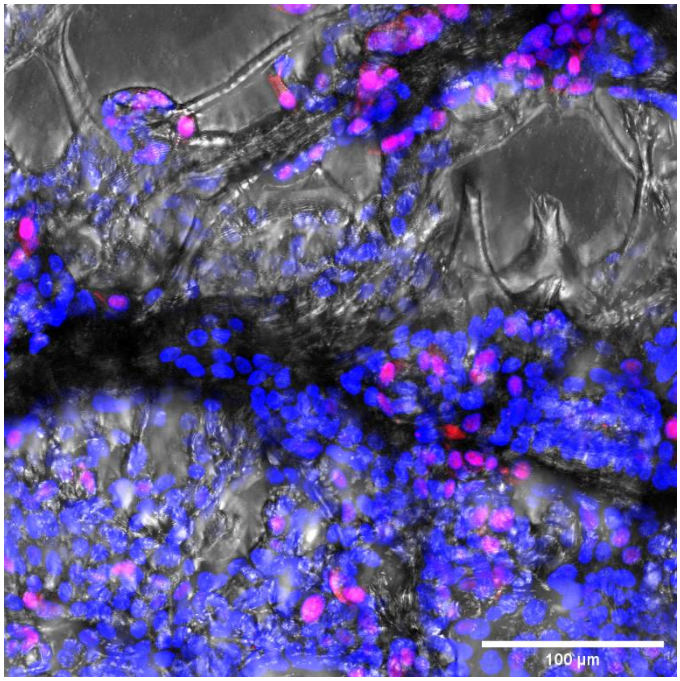

B.

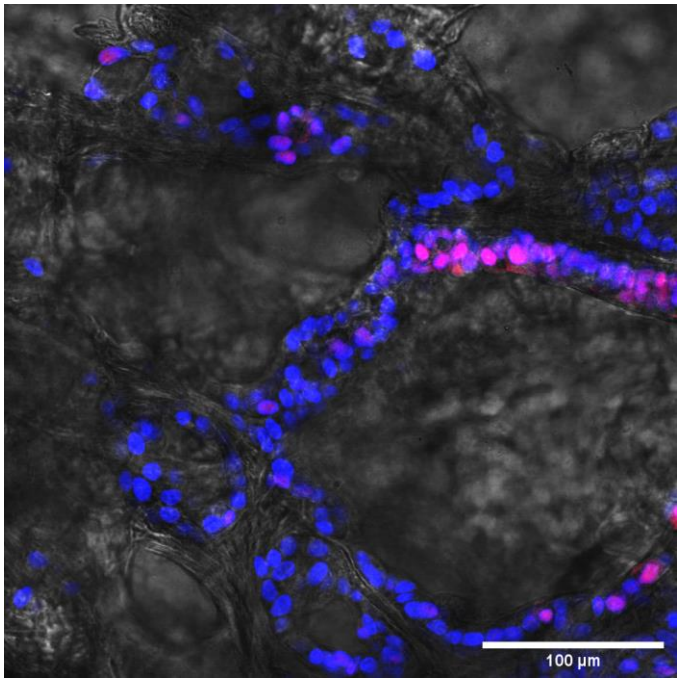

Figure 30: Phase-contrast (grey) images of CCA14 organoids cultured in tumor (CCA2017) scaffolds including DAPI (blue) and Vimentin (red) staining. A: CCA14 organoids cultured in tumor scaffolds with only BM. **B:** CCA14 organoids cultured in tumor scaffolds with branching medium and 20ng/ml TGF-β1. In both cases, cells attached to the scaffold and follow the contour of the ECM.

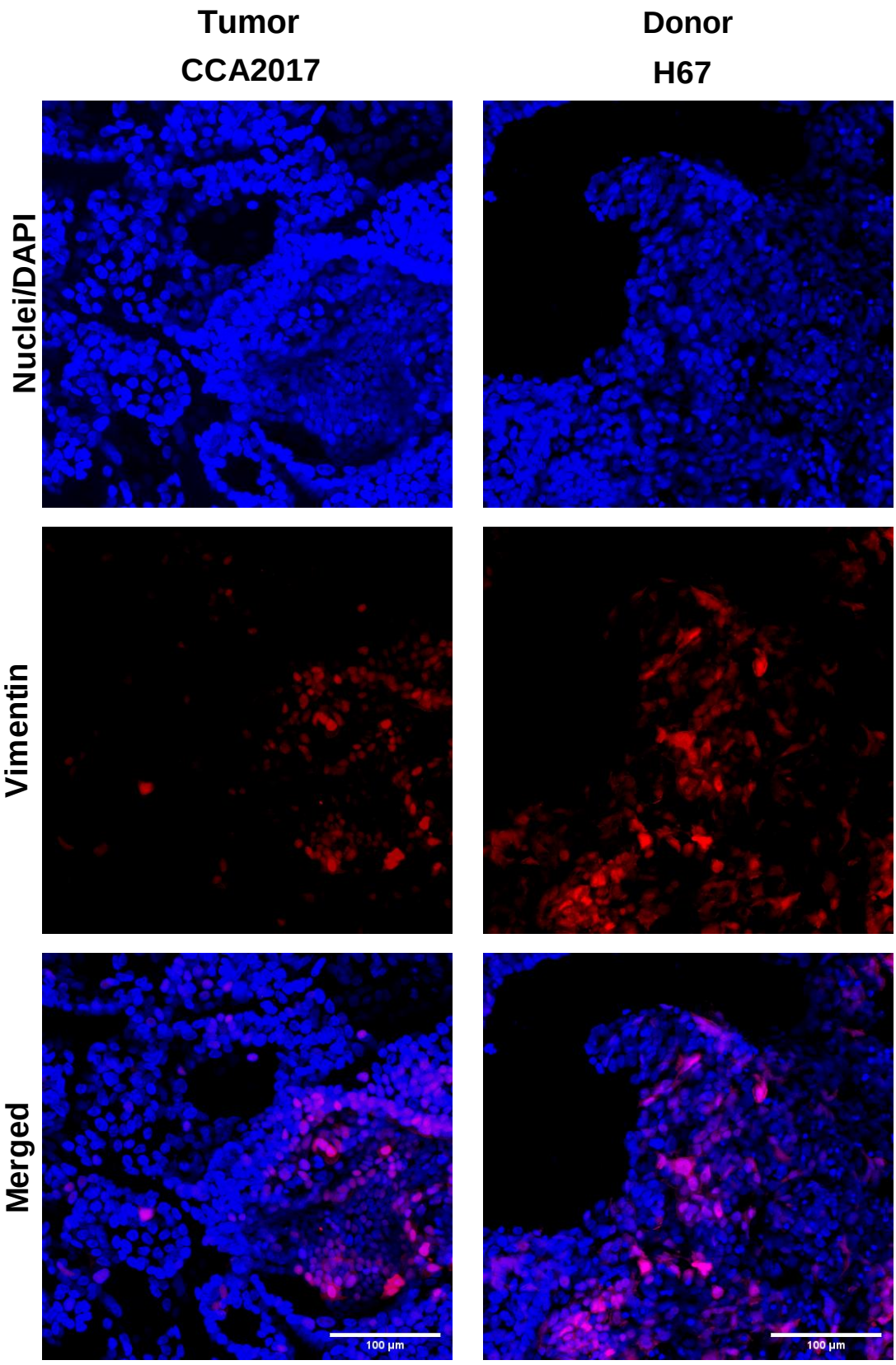

Figure 31: Maximum intensity projection of CCA14 cultured in tumor (CCA2017, left) and donor (H67, right) scaffolds with BM and 20ng/ml TGF-β1. Images represent cell nuclei (Blue/DAPI) and Vimentin (Red) (scale bar is 100µm).

9.8 Gel-gel seeding culture method after 14 days

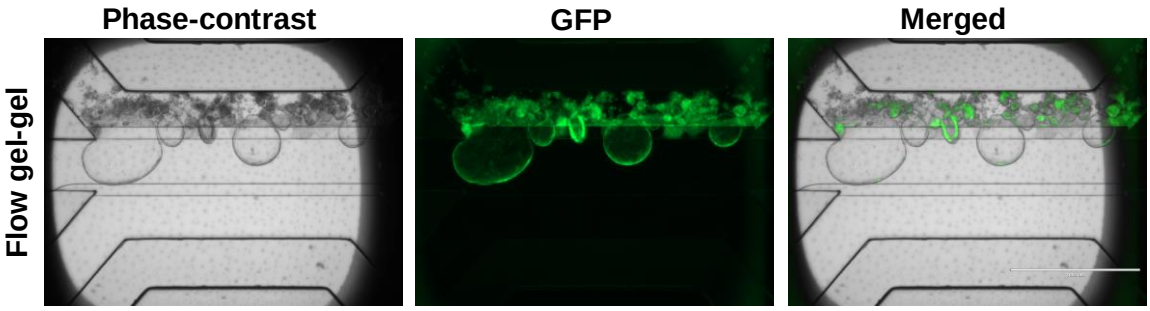

Figure 32: CCA1 organoids tagged with GFP cultured on a chip using the gel-gel seeding culture method for 14 days. Single cells did grow into organoids in the top BME channel. Subsequently, some cells migrated to the middle BME channel, but did not reach the bottom medium channel (scale bar is 1000µm).